NASA CR-72235
UM-06324-4-T

Solution of the Blasius Boundary Layer Equation Behind a Shock with Vaporization and Combustion at the Wall

by

Kenneth W. Ragland

prepared for

NATIONAL AERONAUTICS AND SPACE ADMINISTRATION
Contract NASr 54(07)

July 1967

THE UNIVERSITY OF MICHIGAN
Ann Arbor, Michigan

Requests for copies of this report should be referred to

National Aeronautics and Space Administration
Office of Scientific and Technical Information
Attention: AFSS-A
Washington, D.C. 20546

NASA CR-72235

SOLUTION OF THE BLASIUS BOUNDARY LAYER EQUATION BEHIND A SHOCK WITH VAPORIZATION AND COMBUSTION AT THE WALL

By

Kenneth W. Ragland

prepared for

NATIONAL AERONAUTICS AND SPACE ADMINISTRATION

July 1967

CONTRACT NAsr-54(07)

Technical Management
NASA Lewis Research Center
Cleveland, Ohio
Chemistry and Energy Conversion Division
Bruce J. Clark

Gas Dynamics Laboratories
Department of Aerospace Engineering
THE UNIVERSITY OF MICHIGAN
Ann Arbor, Michigan

ABSTRACT

Solutions of the Blasius boundary layer equation which account for vaporization and combustion on a flat wall behind a normal shock are presented. The solutions, which were obtained on an analog computer, cover a wide range of shock Mach numbers and wall material-gas combinations. Coefficients of mass transfer, drag and heat transfer to the wall are tabulated.

ACKNOWLEDGMENTS

The author wishes to thank Mr. J. D. Warner of the Aerospace Engineering Department for setting up the circuit and logic board for the analog computer, and Dr. E. K. Dabora for his constructive criticism of the manuscript. The Project Supervisor was Professor J. A. Nicholls.

TABLE OF CONTENTS

LIST OF FIGURES

LIST OF TABLES

NOMENCLATURE

A	constant defined by Eq. 7; scale factor (Fig. 2)
B	constant defined by Eq. 28
C_D	mean drag coefficient
C_H	mean heat transfer coefficient
C_M	mean mass transfer coefficient
C_p	specific heat at constant pressure
D	binary diffusion coefficient
f	Blasius function defined by Eq. 22
h	specific enthalpy
h_i^o	standard heat of formation per unit mass of species i at temperature T^o
ΔH	heat of reaction per unit mass
h_L	latent heat of vaporization per unit mass
I	setting of initial condition pots, see Fig. 2
k	coefficient of thermal conductivity
M_i	symbol for chemical species i
M_s	Mach number of normal shock
m	molecular weight
q_w	heat flux to wall per unit area per second
R	scale factor, see Fig. 2
Re	Reynolds number
T	temperature
u	mass average velocity in the x direction (wall fixed coordinates)
$\bar{u}$	mass average velocity in the x direction (shock fixed coordinates)
v	mass average velocity in the y direction
x	distance from shock along the wall
y	distance normal to the wall
Y_i	mass fraction of species i

α	scale factor, see Fig. 2
β	scale factor, see Fig. 2
β_i	defined by Eq. 6
β_T	defined by Eq. 5
γ	scale factor, see Fig. 2; also ratio of specific heats
η	similarity parameter defined by Eq. 19
μ	viscosity
ν_i'	stoichiometric coefficient for species i appearing as a reactant
ν_i''	stoichiometric coefficient for species i appearing as a product
ρ	density
τ_w	shear stress at the wall
ϕ	fuel to oxidizer mass ratio
ψ	stream function defined by Eq. 18

Subscripts

1	conditions upstream of shock
2	conditions in the convective flow outside the boundary layer
f	refers to the fuel species
o	refers to the oxidizer species
s	refers to the shock
w	conditions at the wall

INTRODUCTION

It has recently been discovered that when a shock wave passes over a layer of liquid fuel on the wall of a tube in an oxidizing atmosphere that combustion takes place rapidly enough to reinforce the leading shock wave[1-4]. That is to say, the combustion drives the shock wave in the manner of a detonation. It appears that, initially at least, the combustion takes place within the boundary layer behind the shock wave. While this boundary layer is undoubtedly turbulent almost immediately behind the shock, it is useful to develop a laminar analysis as a basis of comparison with the necessarily less rigorous turbulent analyses. The solution for the laminar case with appropriate assumptions can be obtained from ordinary flat plate boundary layer theory.

The mathematical formulation of the laminar boundary layer on a stationary flat plate in a uniform air stream was given by Prandtl in 1904 and the resulting differential equation was solved by Blasius[5]. Emmons and Leigh[6] extended the formulation and solution of the Blasius boundary layer equation for flow over a flat plate to include mass addition from the plate and combustion within the boundary layer. Mirels[7] obtained the solution of the Blasius equation for the laminar boundary layer behind a shock wave in a shock tube.

The present solution combines the aforementioned works in order to study the laminar boundary layer on a plate with a thin layer of fuel which is exposed to an oxidizing atmosphere and swept over by a normal shock of constant strength. The model for the problem is shown in Fig. 1. The analysis which leads to the Blasius equation with more general boundary conditions than have previously been used is presented along with the solutions. Coefficients of mass transfer, drag and heat transfer to the wall may be obtained from the initial conditions. The complete solutions are of interest for future analysis of the boundary layer profiles.

The mathematical problem is formulated in a coordinate system fixed with respect to the shock. However, the transfer coefficients are defined in terms of the convective velocity relative to the wall. The model for the problem is shown in Fig. 1 in a coordinate system fixed with respect to the shock. The transformation from the laboratory coordinate x to the shock fixed coordinate $\bar{x}$ is given by $\bar{x} = u_s t - x$. The velocity transformation between coordinates is $\bar{u} = u_s - u$.

The following assumptions are made:

1. The flow is laminar, steady, at constant pressure and the usual boundary layer approximations hold.

2. The Prandtl number is unity, the Schmidt number based on binary diffusion coefficients for each pair of species is unity; body forces, radiative energy transport, and thermal diffusion are neglected.

3. $\rho\mu/\rho_2\mu_2 = 1$

4. There is a one step chemical reaction of the form

$$\sum_{i=1}^{N} \nu_i' M_i \rightarrow \sum_{i=1}^{N} \nu_i'' M_i$$

5. The temperature of the vaporizing fuel is constant and equal to the equilibrium boiling point temperature.

6. The properties of the external stream are constant.

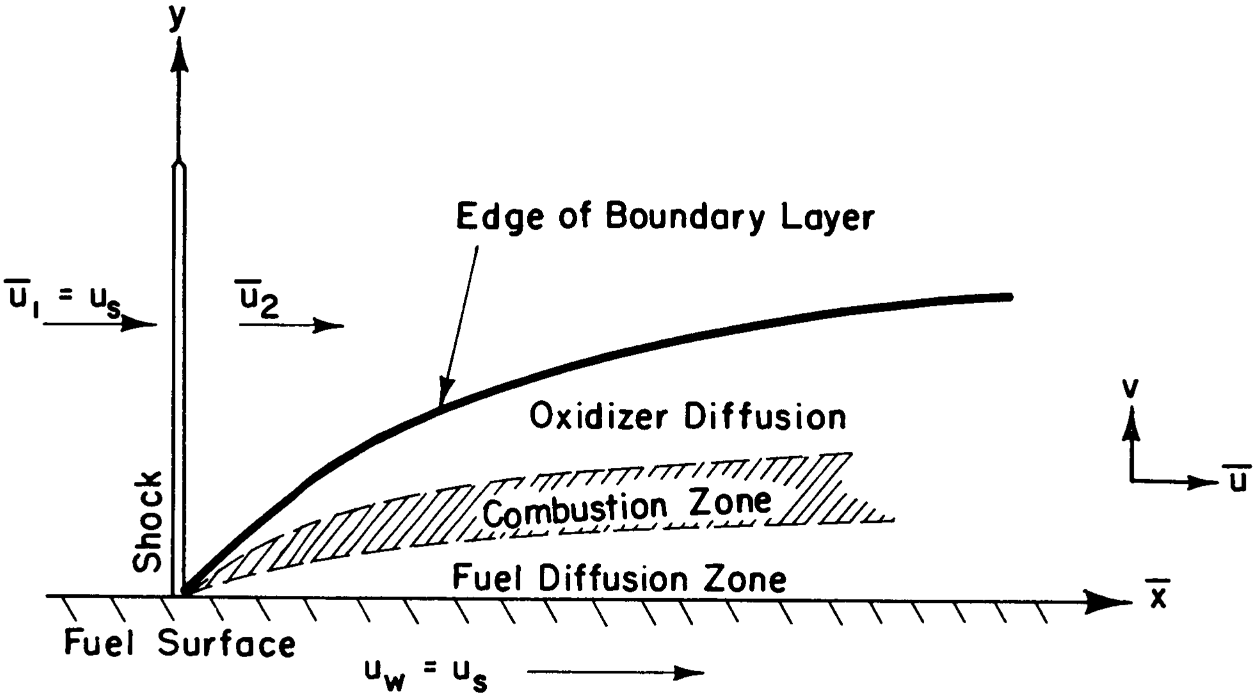

Fig. 1. Boundary layer model and coordinate system fixed with respect to the shock.

FORMULATION OF THE BOUNDARY LAYER EQUATIONS

Under the above assumptions the boundary layer equations in the form given by Williams[8], which is referred to as the Shvab-Zeldovich form, are:

Overall continuity,

$$\frac{\partial \rho \bar{u}}{\partial \bar{x}} + \frac{\partial \rho v}{\partial y} = 0 \tag{1}$$

Momentum,

$$\rho \bar{u} \frac{\partial \bar{u}}{\partial \bar{x}} + \rho v \frac{\partial \bar{u}}{\partial y} = \frac{\partial}{\partial y}\left(A \frac{\partial \bar{u}}{\partial y}\right) \tag{2}$$

Energy,

$$\rho \bar{u} \frac{\partial \beta_T}{\partial \bar{x}} + \rho v \frac{\partial \beta_T}{\partial y} = \frac{\partial}{\partial y}\left(A \frac{\partial \beta_T}{\partial y}\right) \tag{3}$$

Continuity of species

$$\rho \bar{u} \frac{\partial \beta_i}{\partial \bar{x}} + \rho v \frac{\partial \beta_i}{\partial y} = \frac{\partial}{\partial y}\left(A \frac{\partial \beta_i}{\partial y}\right) \tag{4}$$

where

$$\beta_T \equiv \frac{\displaystyle\int_{T^o}^{T} C_p \, dT + \frac{\bar{u}^2}{2}}{\displaystyle\sum_{i=1}^{N} h_i^{\,o} \, m_i \, (\nu_i{}' - \nu_i{}'')} - \frac{Y_1}{m_1 \, (\nu_1{}'' - \nu_1{}')} \tag{5}$$

$$\beta_i \equiv \frac{Y_i}{m_i \, (\nu_i{}'' - \nu_i{}')} - \frac{Y_1}{m_1 \, (\nu_1{}'' - \nu_1{}')} \tag{6}$$

$$A \equiv \rho D_i = \mu = \frac{k}{C_p} \tag{7}$$

and index 1 may represent any particular species; however, it is convenient to have it represent the oxidizer.

In this formulation the reaction rate terms have been eliminated at the expense of obtaining a complete solution for the temperature and composition profiles. However, the velocity profile and the evaporation rate of the fuel layer may be obtained without further loss of generality. This formulation will be sufficient for our present purpose.

The boundary conditions for the energy equation are given by an energy balance at the liquid layer as shown below.

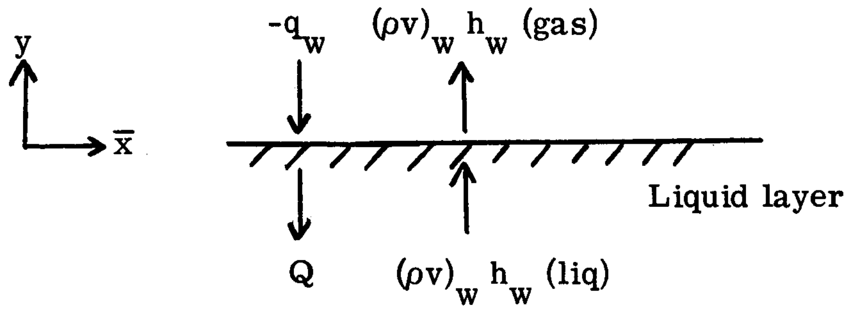

Since the thermal conductivity of liquids is comparatively low, the heat flux through the liquid, Q, is neglected. The heat transfer to the liquid, q_w, is given by:

$$q_w = \left[- k \frac{\partial h}{\partial y} + \rho \sum_{i=1}^{N} D_i \, h_i \, \frac{\partial Y_i}{\partial y} \right]_w$$

As discussed by Lees[9], when the Lewis number is unity (where Le = Sc/Pr), the second term on the right is zero and q_w is independent of the mechanism of heat transfer or the magnitude of the chemical reaction rates. The boundary conditions for the energy equation are then, at $y = 0$, $h = h_w$, which evaluated at the equilibrium boiling temperature of the fuel; and at $y = 0$,

$$k_w \left(\frac{\partial h}{\partial y} \right)_w = (\rho v)_w \, h_L$$

since $h_L = h_w(g) - h_w(\ell)$. At $y = \infty$, $h = h_2$, which is given by the normal shock relations.

In terms of β, the boundary conditions for the energy equations are

at $y = 0$,
$$\beta_T = \beta_{T_w} \tag{8}$$

at $y = 0$,
$$\sum_{i=1}^{N} h_i^o \, m_i \, (\nu_i' - \nu_i'') \left(\frac{\partial \beta_T}{\partial y}\right)_w - u_s \left(\frac{\partial \bar{u}}{\partial y}\right)_w = \frac{C_{p_w} \, (\rho v)_w \, h_L}{k_w} \tag{9}$$

at $y = \infty$,
$$\beta_T = \beta_{T_2} \tag{10}$$

Boundary conditions on the velocity are at $y = \infty$, $\bar{u} = \bar{u}_2$, which is given by tne normal snock relations; and at $y = 0$, $\bar{u} = u_s$, which is the shock velocity. Also at $y = 0$, v must be determined by the vaporization and moving wall conditions as follows. Since the energy equation and the momentum equation have the same form, a particular solution for the energy in terms of the velocity is given by the "Crocco relation,"

$$\beta_T = \left(\frac{\beta_{T_2} - \beta_{T_w}}{\bar{u}_2 - u_s}\right) \bar{u} + \frac{\beta_{T_w} \bar{u}_2 - \beta_{T_2} u_s}{\bar{u}_2 - u_s} \tag{11}$$

and differentiating,

$$\frac{\partial \beta_T}{\partial y} = \left(\frac{\beta_{T_2} - \beta_{T_w}}{\bar{u}_2 - u_s}\right) \frac{\partial \bar{u}}{\partial y} \tag{12}$$

Substituting Eq. (12) into Eq. (9) it is seen that at $y = 0$, v must satisfy the equation

$$\frac{\sum_{i=1}^{N} h_i^o m_i (\nu_i' - \nu_i'') \left(\beta_{T_2} - \beta_{T_w}\right) - \bar{u}_2 u_s + u_s^2}{\bar{u}_2 - u_s} \left(\frac{\partial \bar{u}}{\partial y}\right)_w$$

$$= \frac{(\rho v)_w h_L C_{p_w}}{k_w} \tag{13}$$

In order to solve the momentum equation the first step is to transform the equation to incompressible form by applying the Howarth transformation,

$$z = \int_0^y \rho \, dy \tag{14}$$

$$w = \rho v + \bar{u} \int_0^y \left(\frac{\partial \rho}{\partial \bar{x}}\right) dy \tag{15}$$

Then Eqs. (1) and (2) can be shown to reduce to

$$\frac{\partial \bar{u}}{\partial \bar{x}} + \frac{\partial w}{\partial z} = 0 \tag{16}$$

$$\bar{u} \frac{\partial \bar{u}}{\partial \bar{x}} + w \frac{\partial \bar{u}}{\partial z} = \rho_2 \mu_2 \frac{\partial^2 \bar{u}}{\partial z^2} \tag{17}$$

Next introduce a stream function ψ and a similarity parameter η,

$$\psi = \sqrt{\bar{u}_2 \rho_2 \mu_2 \bar{x}} \, f(\eta) \tag{18}$$

$$\eta = \frac{z}{2}\sqrt{\frac{\bar{u}_2}{\rho_2\,\mu_2\,\bar{\bar{x}}}} \tag{19}$$

Then,

$$\bar{u} = \frac{1}{2}\,\bar{u}_2\,\frac{df}{d\eta} \tag{20}$$

$$\rho v = \frac{1}{2}\sqrt{\frac{\bar{u}_2\,\rho_2\,\mu_2}{\bar{\bar{x}}}}\left(\eta\,\frac{df}{d\eta} - f\right) - \frac{1}{2}\,\bar{u}_2\,\frac{df}{d\eta}\int_0^y \frac{\partial\rho}{\partial\bar{\bar{x}}}\,dy \tag{21}$$

and we obtain the Blasius equation,

$$\frac{d^3f}{d\eta^3} + f\,\frac{d^2f}{d\eta^2} = 0 \tag{22}$$

with the boundary conditions

$$\left(\frac{df}{d\eta}\right)_w = \frac{2u_s}{\bar{u}_2} \tag{23}$$

$$\left(\frac{df}{d\eta}\right)_\infty = 2 \tag{24}$$

$$\frac{f_w}{\left(\dfrac{d^2f}{d\eta^2}\right)_w} = -\,\frac{B}{2\left(1 - \dfrac{u_s}{\bar{\bar{u}}_2}\right)} \tag{25}$$

where

$$B = \frac{\sum h_i^{\,o}\,m_i\,(\nu_i{}' - \nu_i{}'')\,\left(\beta_{T_2} - \beta_{T_w}\right) - \bar{u}_2\,u_s + u_s^{\,2}}{h_L} \tag{26}$$

or substituting the definition of β_T from Eq. (5) and denoting the free stream oxidizer by the subscript o the expression for B becomes,

$$h_L B = \int_{T^o}^{T_2} C_p \, dT - \int_{T^o}^{T_w} C_p \, dT + \frac{\bar{u}_2^{\,2}}{2} + \frac{u_s^{\,2}}{2} - \bar{u}_2 u_s + \frac{Y_{o_2} \sum_{i=1}^{N} h_i^o m_i (\nu_i' - \nu_i'')}{m_o (\nu_o' - \nu_o'')} \tag{27}$$

The last term of Eq. (A. 27) may be rewritten as,

$$Y_{o_2} \left[\frac{m_f (\nu_f' - \nu_f'')}{m_o (\nu_o' - \nu_o'')} \right] \left[\frac{\sum_{i=1}^{N} h_i^o m_i (\nu_i' - \nu_i'')}{m_f (\nu_f' - \nu_f'')} \right]$$

The first bracket is the fuel to oxidizer ratio, ϕ, while the second bracket is the heat of reaction, ΔH. Finally, assuming constant specific heats the expression for B reduces to

$$h_L B = C_{p_2} T_2 - C_{p_w} T_w + Y_{o_2} \phi \, \Delta H + \frac{1}{2} u_2^{\,2} \tag{28}$$

The coefficients of mass addition, drag and heat transfer as a function of B and $u_s/\bar{u}_2$ may be obtained from the solution of the initial conditions for f and f''. It should be noted that q_w is related to τ_w by the Reynolds analogy which holds rigorously under the assumptions previously listed. This can be shown as follows. Differentiating Eq. (5) and equating it to Eq. (12) yields

$$\frac{\frac{\partial h}{\partial y} + \bar{u}\,\frac{\partial \bar{u}}{\partial y}}{\sum_{i=1}^{N} h_i^{\,o}\, m_i\,(\nu_i' - \nu_i'')} = \left(\frac{\beta_{T_2} - \beta_{T_w}}{\bar{u}_2 - u_s}\right)\frac{\partial \bar{u}}{\partial y} \tag{29}$$

Substituting the definition of β_T and rearranging,

$$\frac{\partial h}{\partial y} + \bar{u}\,\frac{\partial \bar{u}}{\partial y} = \frac{\partial \bar{u}}{\partial y}\left[C_{p_2} T_2 + \frac{\bar{u}_2^{\,2}}{2} - \frac{Y_{O_2}\sum_{i=1}^{N} h_i^{\,o}\, m_i\,(\nu_i' - \nu_i'')}{m_i\,(\nu_i'' - \nu_i')} - C_{p_w} T_w - \frac{u_s^{\,2}}{2}\Bigg/ \bar{u}_2 - u_s\right] \tag{30}$$

Since $q_w = -\,\mu_w\,(\partial h/\partial y)_w$, Eq. (33) becomes,

$$q_w = -\,\tau_w\left[\frac{C_{p_2} T_2 - C_{p_w} T_w + \frac{1}{2}\,(\bar{u}_2 - u_s)^2 + Y_{O_2}\,\phi\,\Delta H}{\bar{u}_2 - u_s}\right] \tag{31}$$

Integrating q_w and τ_w over $\bar{x}$ and dividing by $\bar{x}\rho_2 u_2$,

$$\frac{\int_0^{\bar{x}} q_w \, d\bar{x}}{\bar{x}\rho_2 u_2} = \frac{C_D}{2}\left[C_{p_2} T_2 + \frac{u_2^2}{2} + Y_{o_2} \phi \Delta H - C_{p_w} T_w\right] \tag{32}$$

or,

$$C_H = \frac{C_D}{2} \tag{33}$$

where the mean transfer coefficients are defined as,

$$C_M = \frac{\int_0^{\bar{x}} \rho_w v_w \, d\bar{x}}{\bar{x}\rho_2 u_2} \tag{34}$$

$$C_D = \frac{\mu_w \int_0^{\bar{x}} \left(\frac{\partial u}{\partial y}\right)_w d\bar{x}}{\bar{x} \frac{1}{2} \rho_2 u_2^2} \tag{35}$$

$$C_H = \frac{\int_0^{\bar{x}} q_w \, d\bar{x}}{\bar{x} \rho_2 u_2 \left(C_{p_2} T_2 + \frac{u_2^2}{2} + Y_{o_2} \phi \Delta H - C_{p_w} T_w\right)} \tag{36}$$

Next it is convenient to introduce a Reynolds number* defined following Glass and Hall[10] such that,

$$\mathrm{Re}_2 = \frac{\rho_2 u_2^2 x}{\mu_2 \bar{u}_2} \tag{37}$$

The transfer coefficients may be expressed in terms of the Blasius function by introducing Eq. (20), (21), and (39) into (33)-(35),

$$C_M \sqrt{\mathrm{Re}_2} = - f(0) \tag{38}$$

$$C_D \sqrt{\mathrm{Re}_2} = \frac{|f''(0)|}{(u_s/\bar{u}_2 - 1)} \tag{39}$$

$$C_H \sqrt{\mathrm{Re}_2} = \frac{|f''(0)|}{2(u_s/\bar{u}_2 - 1)} \tag{40}$$

*This definition, which is slightly different than used in Ref. 3, is the appropriate one for comparison to a stationary flat plate.

SOLUTION

The differential Eq. (22) with boundary conditions (23, 24, and 25) is to be solved. When $u_s = B = 0$ we have the original Blasius equations for a stationary flat plate with no mass additions. When $u_s = 0$ and B is finite we have the Emmons' problem. And when $B = 0$ and u_s is finite we have the shock tube equations solved by Mirels. Since the differential equation is third order non-linear, the combined two parameter set of boundary conditions necessitates that the problem be solved anew. Because we have a two point boundary value problem in which the starting conditions are not known explicitly for physically interesting cases until the solution is obtained, the equations were solved numerically on an analog rather tnan a digital computer. The University of Michigan 90 amplifier hybrid analog computer was used with the network shown in Fig. 2. The computer was programmed to solve the equations repetitively so that the effect of varying the initial condition pots in order to satisfy the solution at "infinity" was immediately apparent, and in this manner boundary condition (25) could be obtained. The initial voltages which were used on the integrating amplifiers and the appropriate scale factors to achieve full scale deflections are shown in Table I.

The results of the initial conditions which were obtained as solutions to Eq (22) are shown in Table II. Also shown are the transfer coefficients which may be obtained from the solutions. Twenty-seven cases were solved. Cases 1, 2, 3, 10, 16, and 22 were a repeat of previously known solutions in order to provide a check on the technique. Four different velocity ratios ($u_s/\bar{u}_2$), which represented shock Mach numbers of 1. 58, 2. 24, 3. 16 and 5. 00 for a gas with a ratio of specific heats of 1. 4, were considered. At each velocity ratio the parameter B was varied to cover a range of 0 to at least 70. For convenience f(0) and f''(0) are plotted versus B for the various f'(0)'s in Fig. 3 and 4.

The output from the analog computer for each set of initial conditions shown in Table II (cases 1-27) is compiled in Fig. 5. The time axes on the recorder becomes η, and the function f and its three derivatives are recorded as a function of η. The η scale is shown only for the first case but can be determined for the other cases from the timing marker of the recorder (i. e., the distance between marks is equivalent to $\Delta\eta = 1$). The position of $\eta = 0$ is indicated by the discontinuity in slope of the curve. The third derivative is shown to indicate the accuracy of the 37 segment multiplier unit.

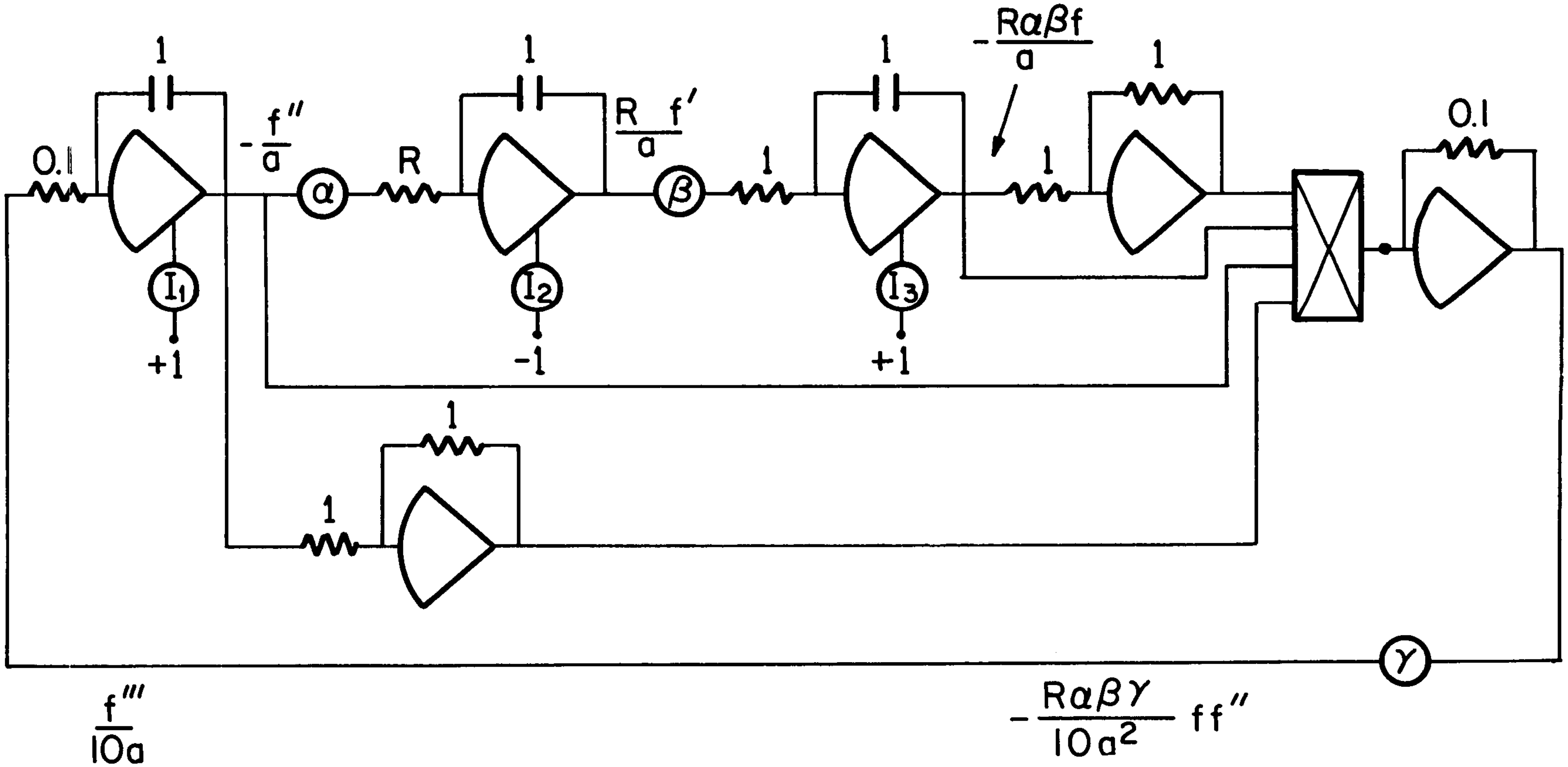

Fig. 2. Circuit used on the analog computer.

TABLE I. SUMMARY OF THE CONSTANTS USED WITH THE ANALOG CIRCUIT SHOWN IN FIG. 2

Case	a	R	α	β	γ	I_1	I_2	$-I_3$
1	1. 5	1	. 7500	. 2000	1	-88. 53	0	0
2	1. 5	1	. 7500	. 2000	1	- 9. 473	0	10. 00
3	3	1	. 7500	. 4000	1	96. 08	100. 0	0
4	3	1	. 7500	. 4000	1	59. 19	100. 0	10. 00
5	3	1	. 7500	. 4000	1	32. 09	100. 0	20. 00
6	1. 5	1	. 3750	. 4000	1	30. 09	100. 0	30. 00
7	1. 5	1	. 3750	. 4000	1	19. 10	100. 0	35. 00
8	1. 5	1	. 3750	. 4000	1	11. 35	100. 0	40. 00
9	1. 5	1	. 3750	. 4000	1	4. 90	100. 0	47. 29
10	8	0. 1	. 1333	1	. 6000	84. 90	100. 0	0
11	6	1	1	1	. 6000	27. 80	100. 0	50. 00
12	6	1	1	1	. 6000	19. 35	100. 0	60. 00
13	6	1	1	1	. 6000	12. 95	100. 0	70. 00
14	6	1	1	1	. 6000	8. 24	100. 0	80. 00
15	6	1	1	1	. 6000	5. 08	100. 0	90. 00
16	12	0. 1	. 1500	1	. 8000	95. 75	100. 0	0
17	6	1	. 7500	1	. 8000	34. 75	100. 0	50. 00
18	6	1	. 7500	1	. 8000	21. 50	100. 0	60. 00
19	6	1	. 7500	1	. 8000	16. 64	100. 0	65. 00
20	6	1	. 7500	1	. 8000	12. 70	100. 0	70. 00
21	6	1	. 7500	1	. 8000	7. 08	100. 0	80. 00
22	20	0. 1	. 2000	1	1	84. 45	100. 0	0
23	10	1	1	1	1	36. 29	100. 0	40. 00
24	10	1	1	1	1	21. 23	100. 0	50. 00
25	10	1	1	1	1	11. 54	100. 0	60. 00
26	10	1	1	1	1	5. 80	100. 0	70. 00
27	10	1	1	1	1	4. 00	100. 0	75. 00

TABLE II. SUMMARY OF INITIAL CONDITIONS SATISFYING THE BLASIUS EQUATION FOR VARIOUS VALUES OF M_s AND B

Case	-f(0)	f'(0)	-f''(0)	B	M_s	$C_M \sqrt{Re_2}$	$C_D \sqrt{Re_2}$	$C_H \sqrt{Re_2}$
1	0	0	-1.33	0	-	0	1.33	0.67
2	1.00	0	-0.14	14.2	-	1.00	0.14	0.07
3	0	4	2.88	0	1.58	0	2.88	1.44
4	1.00	4	1.77	1.1	1.58	1.00	1.77	0.885
5	2.00	4	0.96	4.1	1.58	2.00	0.96	0.48
6	3.00	4	0.45	13.3	1.58	3.00	0.45	0.225
7	3.50	4	0.29	24.2	1.58	3.50	0.29	0.145
8	4.00	4	0.17	47.1	1.58	4.00	0.17	0.085
9	4.73	4	0.073	130	1.58	4.73	0.073	0.037
10	0	6	6.79	0	2.24	0	3.40	1.70
11	3.00	6	1.67	7.2	2.24	3.00	0.83	0.41
12	3.60	6	1.16	12.4	2.24	3.60	0.58	0.29
13	4.20	6	0.78	21.5	2.24	4.20	0.39	0.19
14	4.80	6	0.49	39.2	2.24	4.80	0.24	0.12
15	5.40	6	0.30	72.0	2.24	5.40	0.15	0.08
16	0	8	11.49	0	3.16	0	3.83	1.91
17	4.00	8	2.08	11.5	3.16	4.00	0.69	0.34
18	4.80	8	1.29	22.3	3.16	4.80	0.43	0.21
19	5.20	8	1.00	31.2	3.16	5.20	0.33	0.16
20	5.60	8	0.76	44.2	3.16	5.60	0.25	0.12
21	6.40	8	0.42	91.4	3.16	6.40	0.14	0.07
22	0	10	16.89	0	5.00	0	4.22	2.11
23	4.00	10	3.63	8.8	5.00	4.00	0.91	0.45
24	5.00	10	2.12	18.9	5.00	5.00	0.53	0.26
25	6.00	10	1.15	41.7	5.00	6.00	0.29	0.14
26	7.00	10	0.58	96.6	5.00	7.00	0.14	0.07
27	7.50	10	0.40	150	5.00	7.50	0.10	0.05

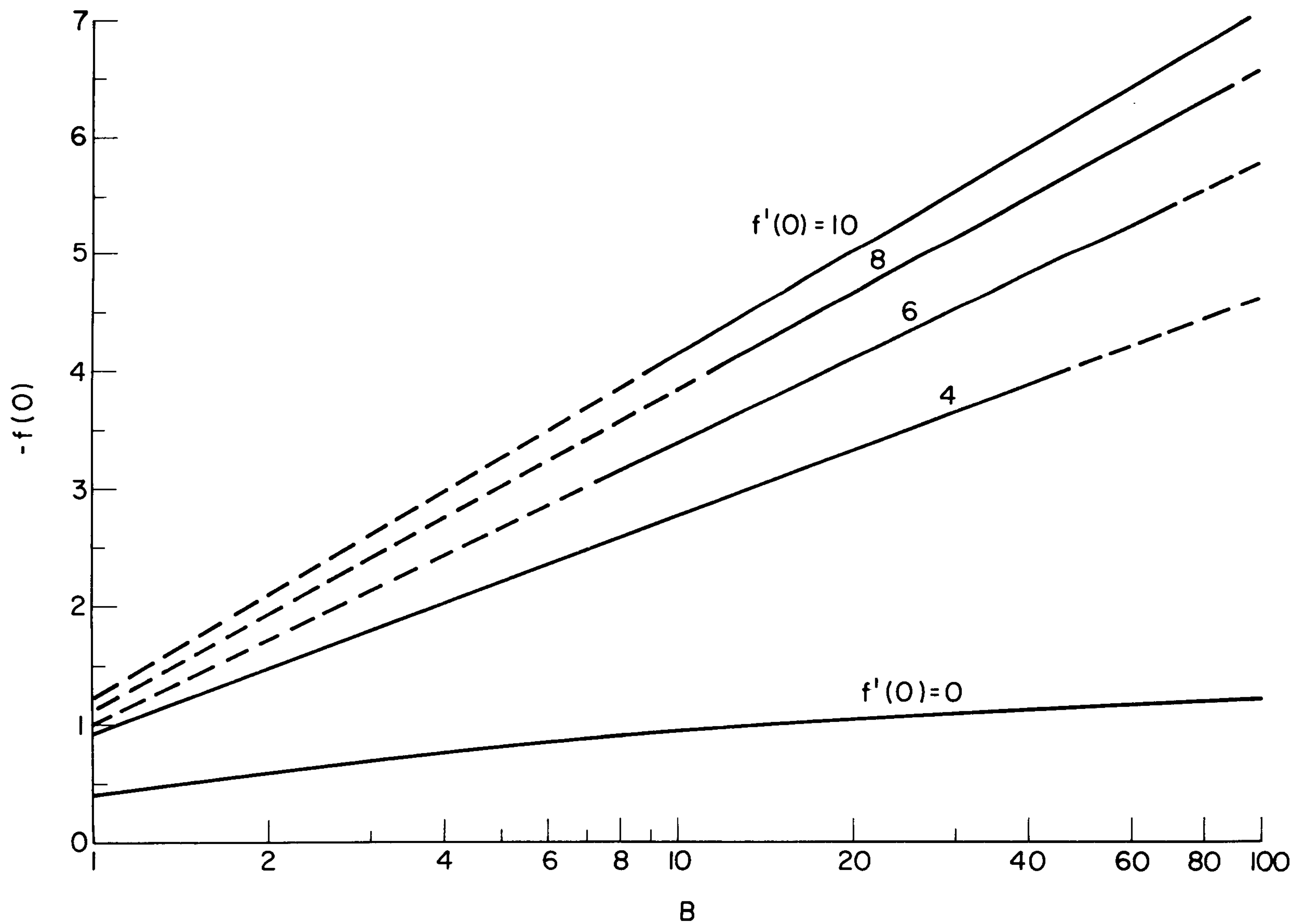

Fig. 3. Initial solutions of the Blasius equation: f(0) vs B for various f'(0).

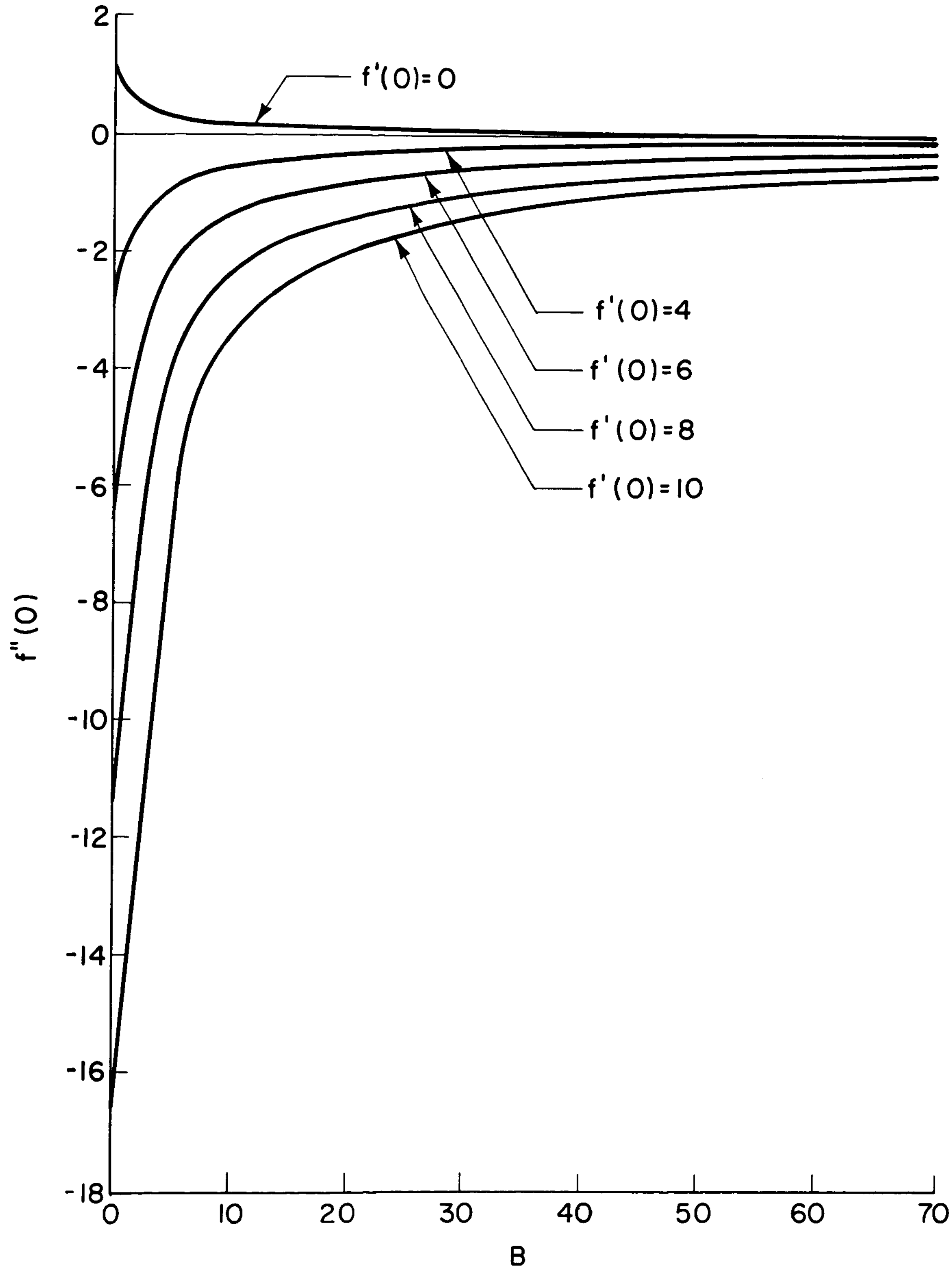

Fig. 4. Initial solutions of the Blasius equation: f"(0) vs B for various f'(0).

DISCUSSION OF THE RESULTS

As indicated in Figs. 3 and 4, $f(0)$ and $f''(0)$ are very strong functions of the thermodynamic parameter B and also, strong functions of the velocity ratio $f'(0)$. Increasing the enthalpy difference between the free stream and the wall, and increasing the heat release within the boundary layer cause $f''(0)$ to decrease in magnitude towards zero and cause $f(0)$ to increase towards a finite limit. The curves for $f'(0) = 0$ represent the solution obtained by Emmons and Leigh. As pointed out by them, increasing B causes the boundary layer to increase in thickness until finally the boundary layer is "blown off," at which point $f(0)$ approaches the limit of 1.238. The effect of the shock fixed coordinate system is to extend this limit.

As is well known, the effect of mass addition due to vaporization and combustion on a flat plate is to greatly reduce the drag coefficient. The boundary layer behind a shock also exhibits this behavior although to a slightly less degree. The drag coefficient for the shock case is considerably higher than for the stationary flat plate, for the same Reynolds number, however. For a B = 5, which is representative of vaporization alone, the drag is reduced by a factor of 3, while for a B = 30, which is representative of vaporization and combustion, the drag is reduced by a factor of 10.

Referring to Fig. 5, the effect of mass addition is to increase the thickness of the boundary, as evidenced by the fact that f' approaches its asymptotic value at a larger value of η as f(0) is increased. The effect of increasing the velocity ratio $u_s/\overline{u}_2$, or equivalently M_s, is to reduce the boundary layer thickness. Also, the effect of increasing f(0) is to cause an inflection of the boundary layer velocity profile. The point of inflection may be located by observing the maximum point of the f'' curve. The effect of increasing the velocity ratio $u_s/\overline{u}_2$ is to suppress this inflection point.

Fig. 5. Solution of the Blasius equation for the 27 cases listed in Table II. (Note: The initial conditions are held until $\eta = 0$ where the solution starts. The position of $\eta = 0$ is indicated by the discontinuity in slope of the curves. The η scale is shown explicitly only for case 1, but it may be determined from the timing markers at the bottom of the page for the other cases.)

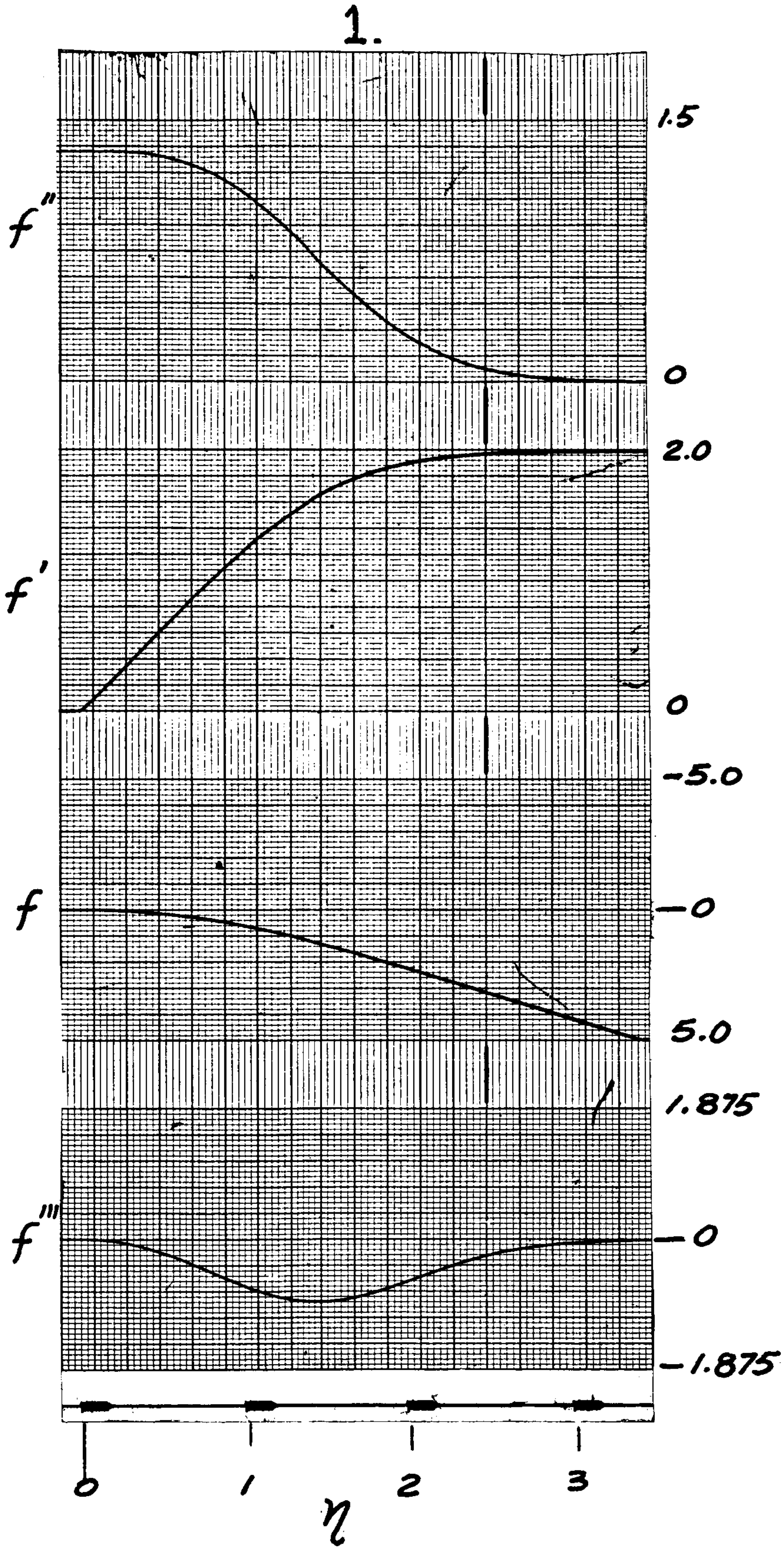

Fig. 5.

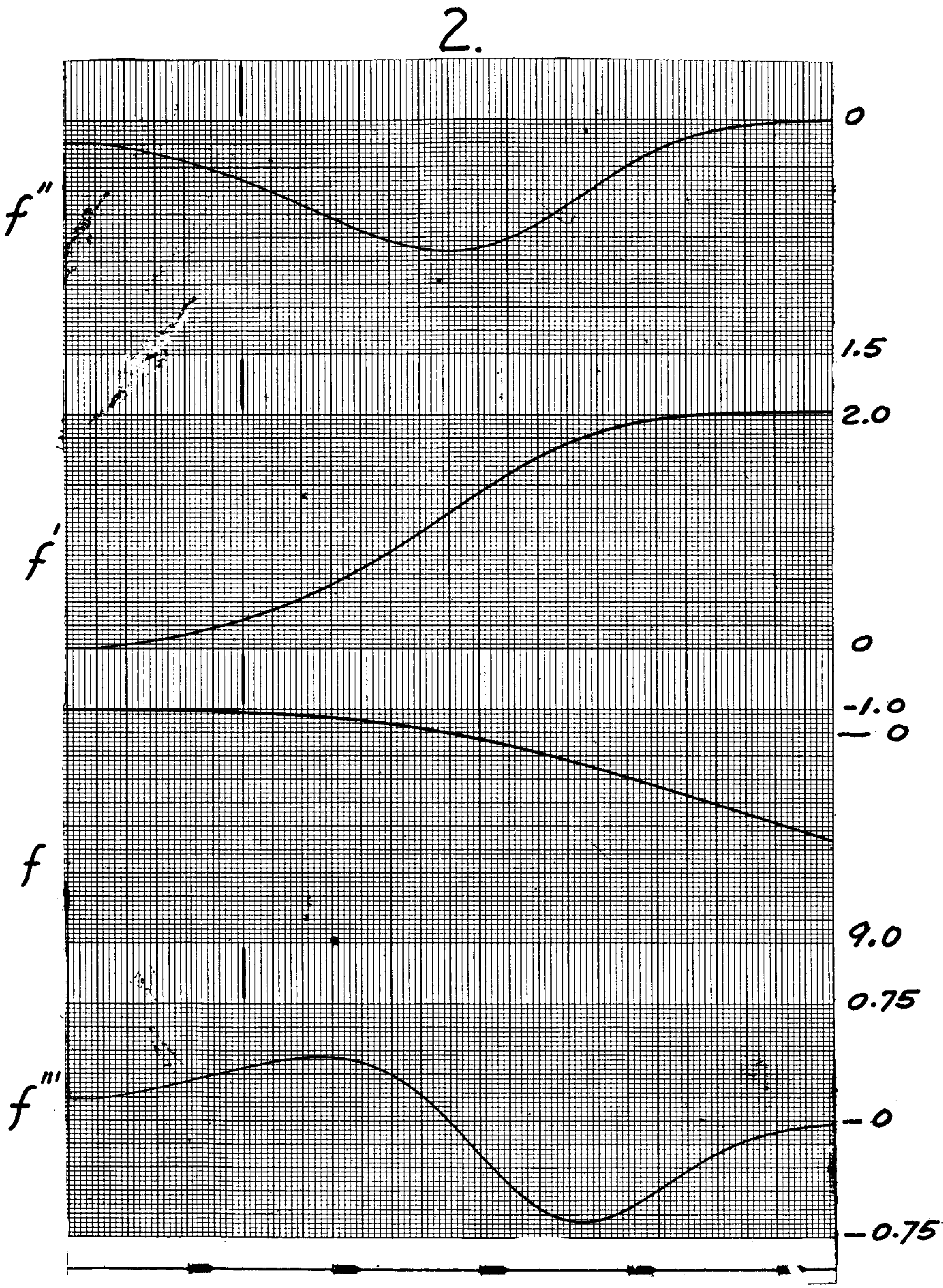

Fig. 5. (Continued)

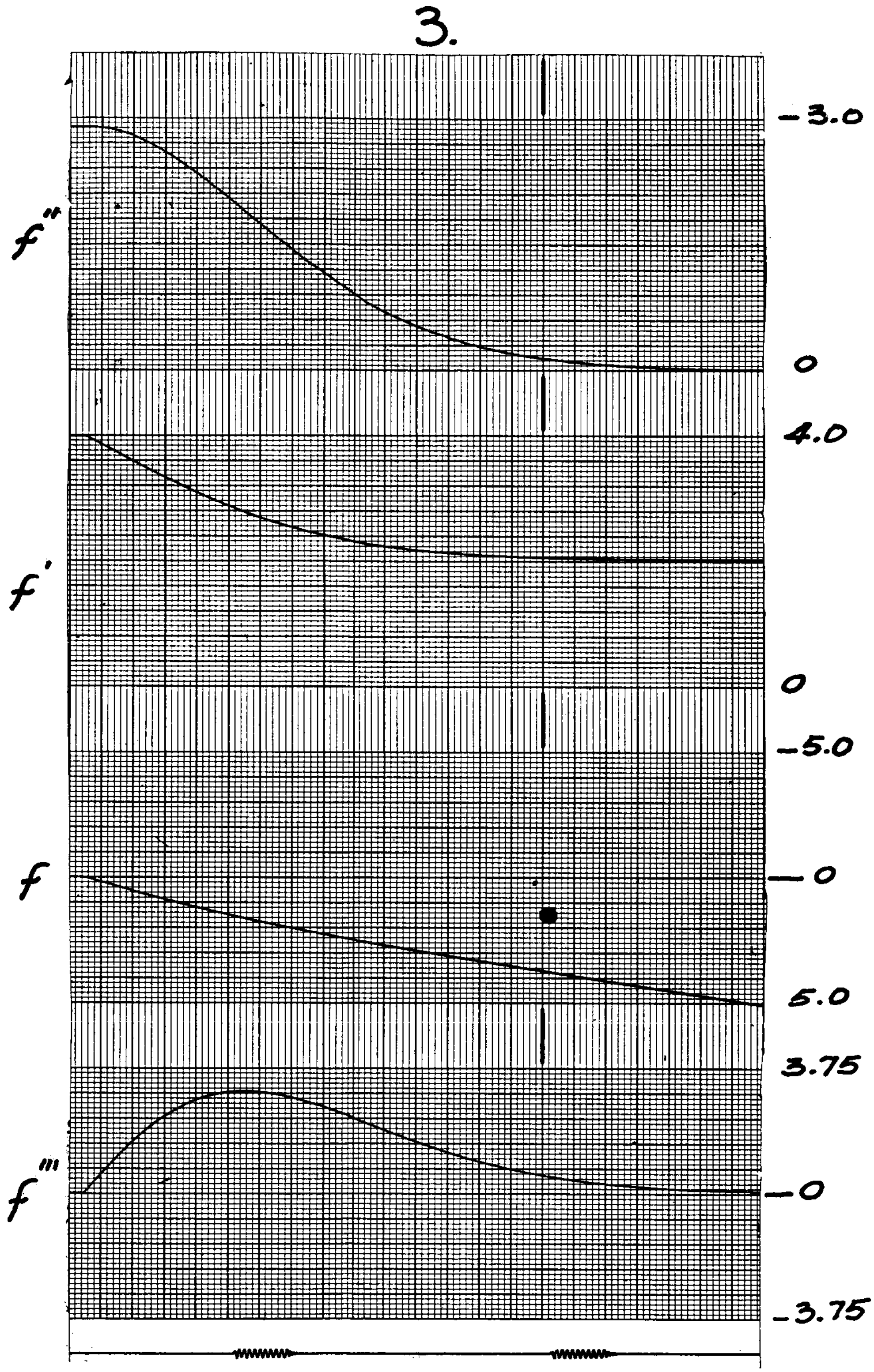

Fig. 5. (Continued)

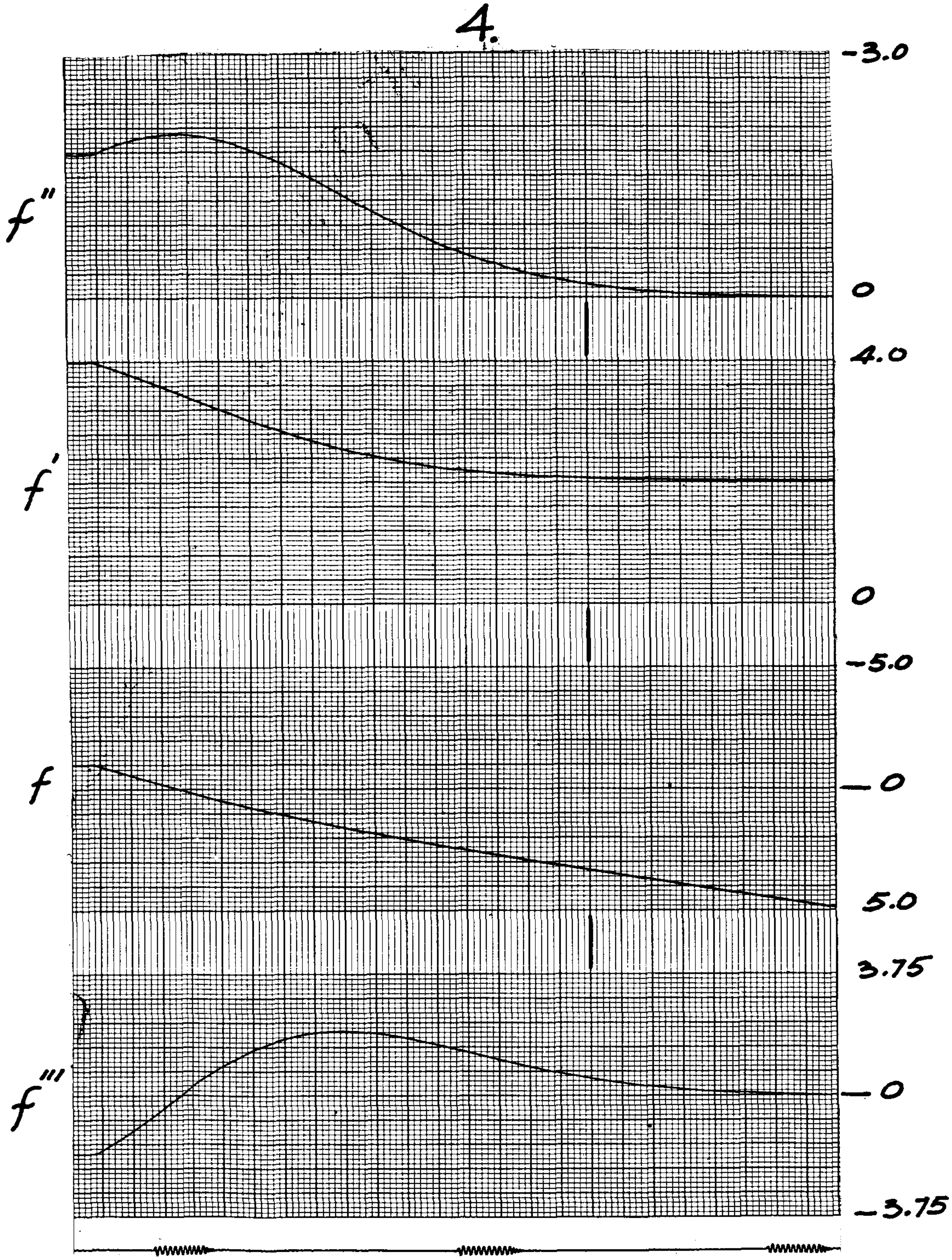

Fig. 5. (Continued)

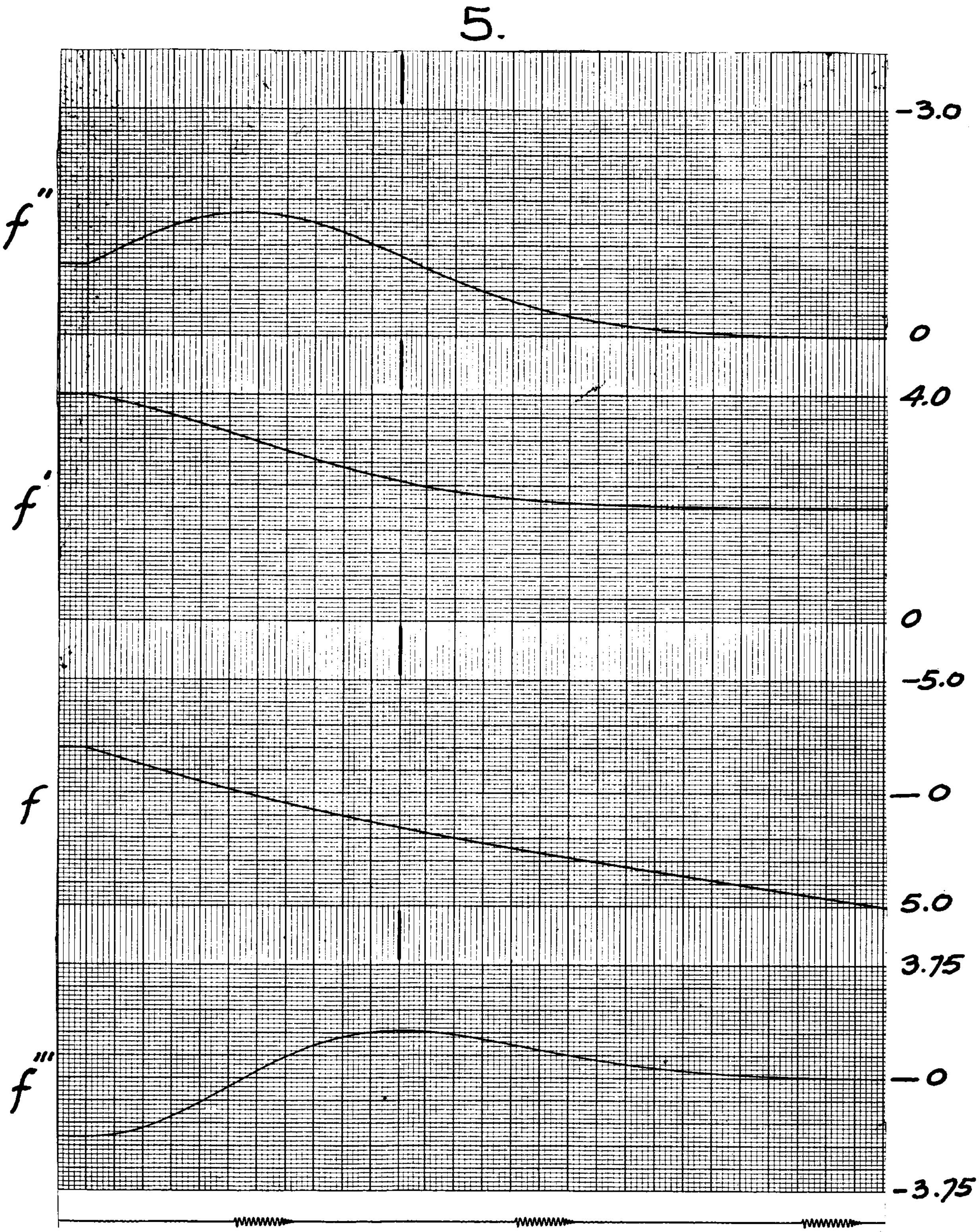

Fig. 5. (Continued)

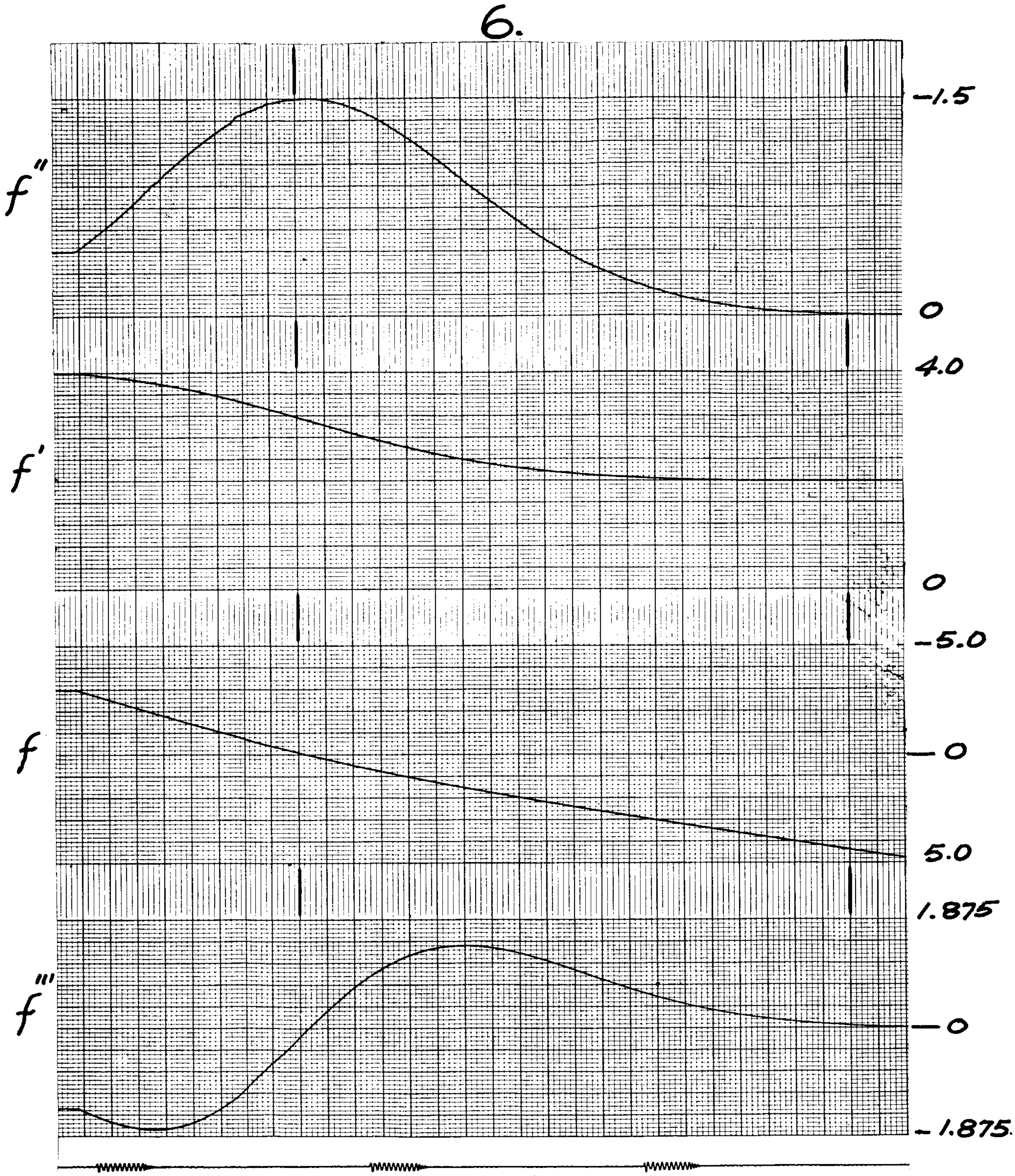

Fig. 5. (Continued)

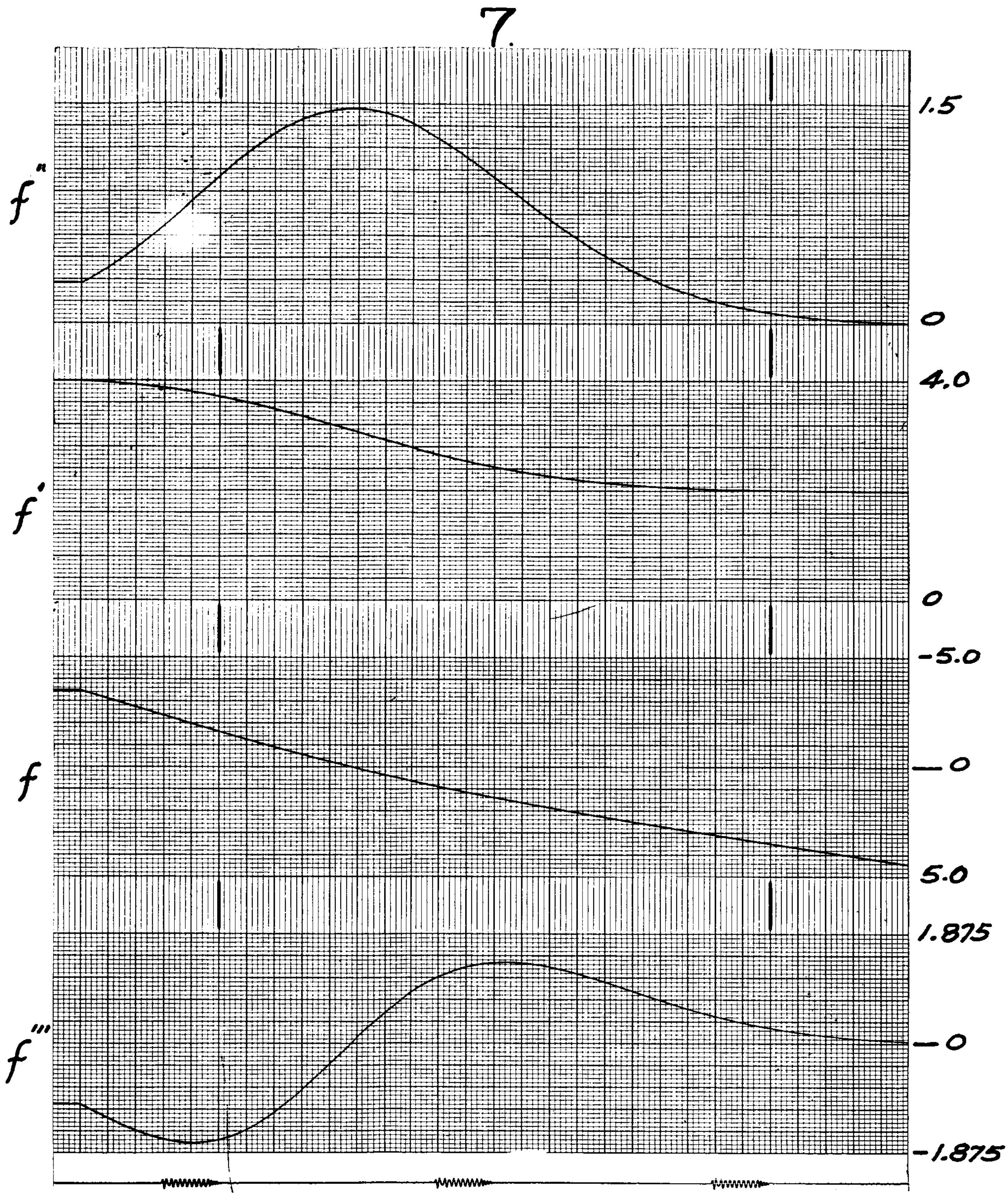

Fig. 5. (Continued)

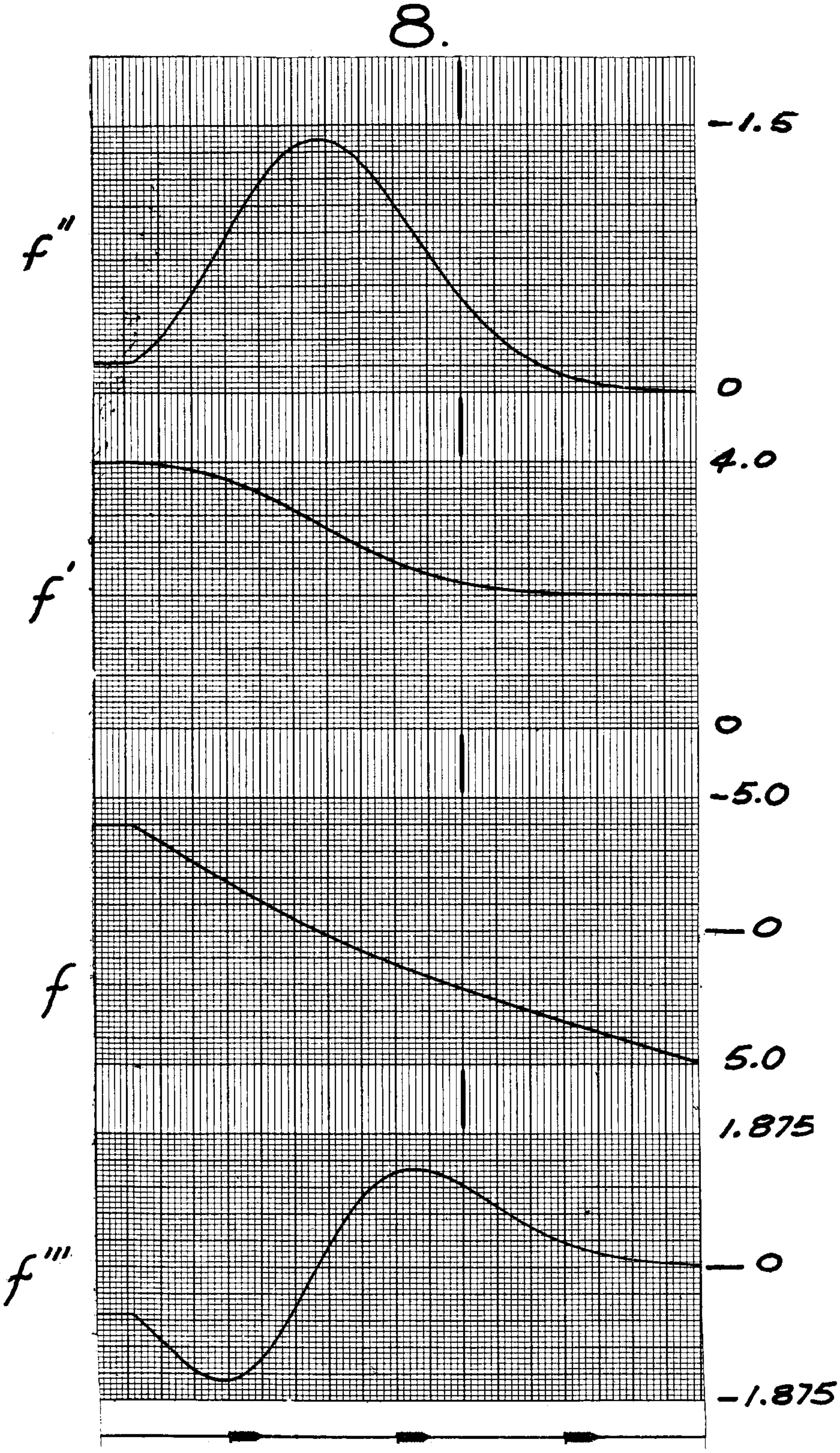

Fig. 5. (Continued)

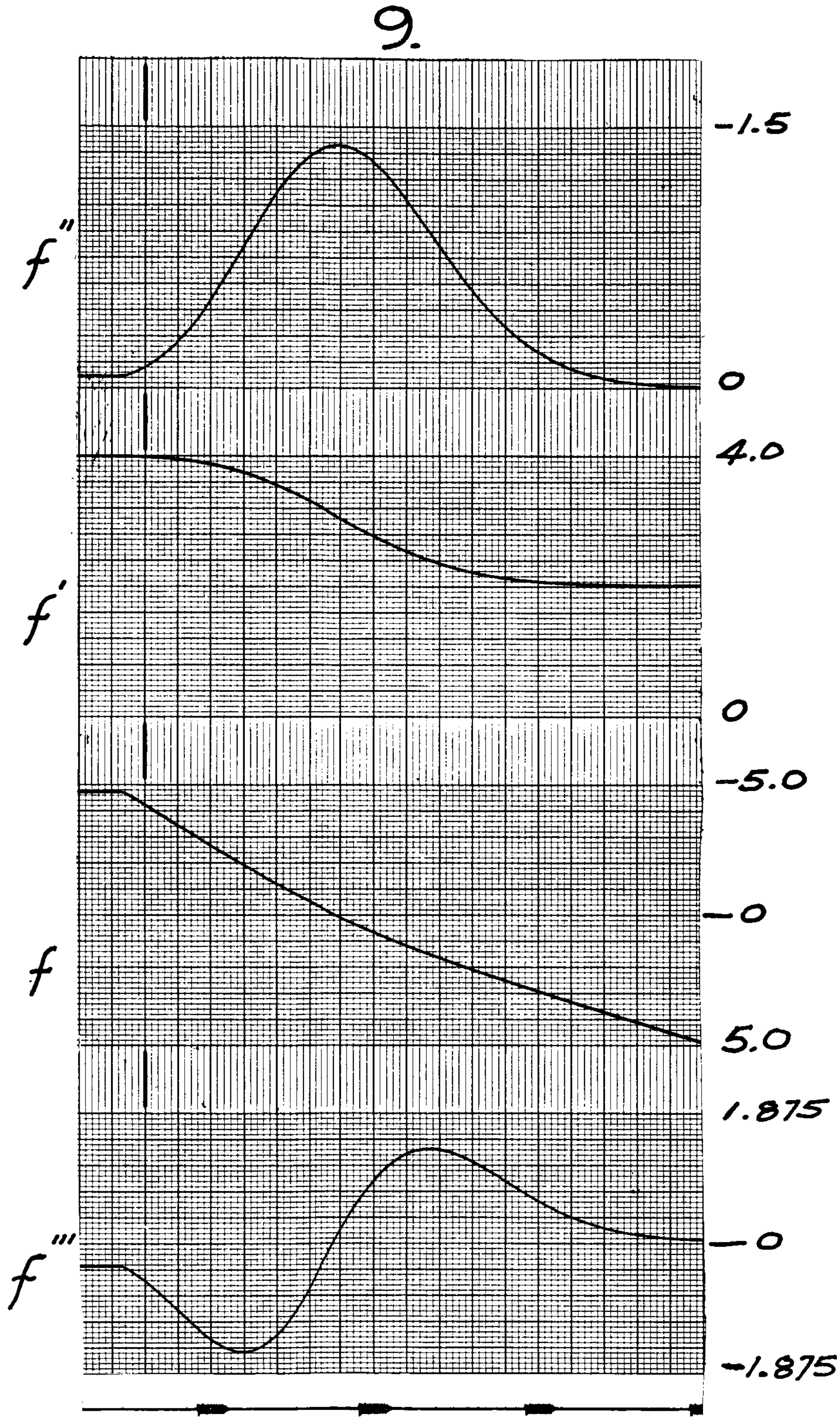

Fig. 5. (Continued)

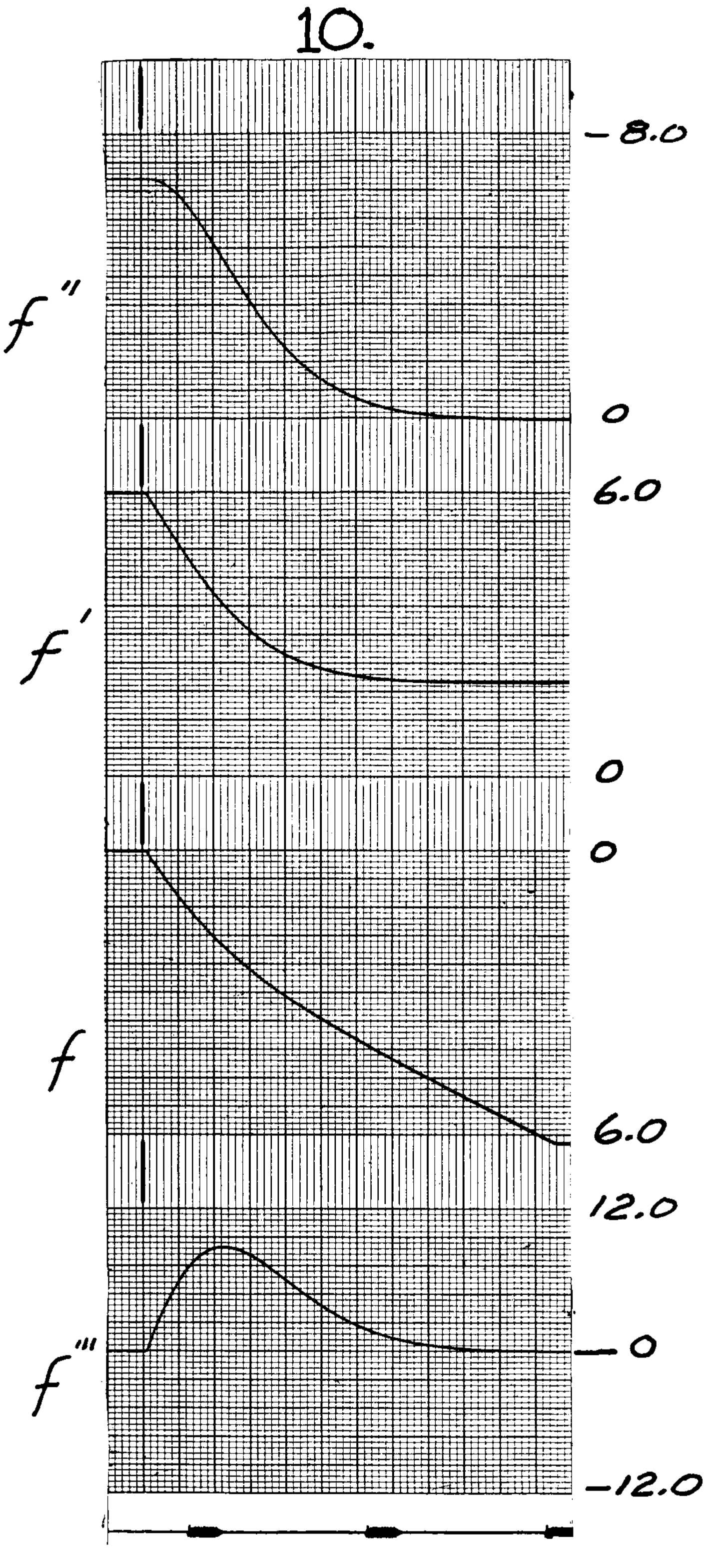

Fig. 5. (Continued)

11.

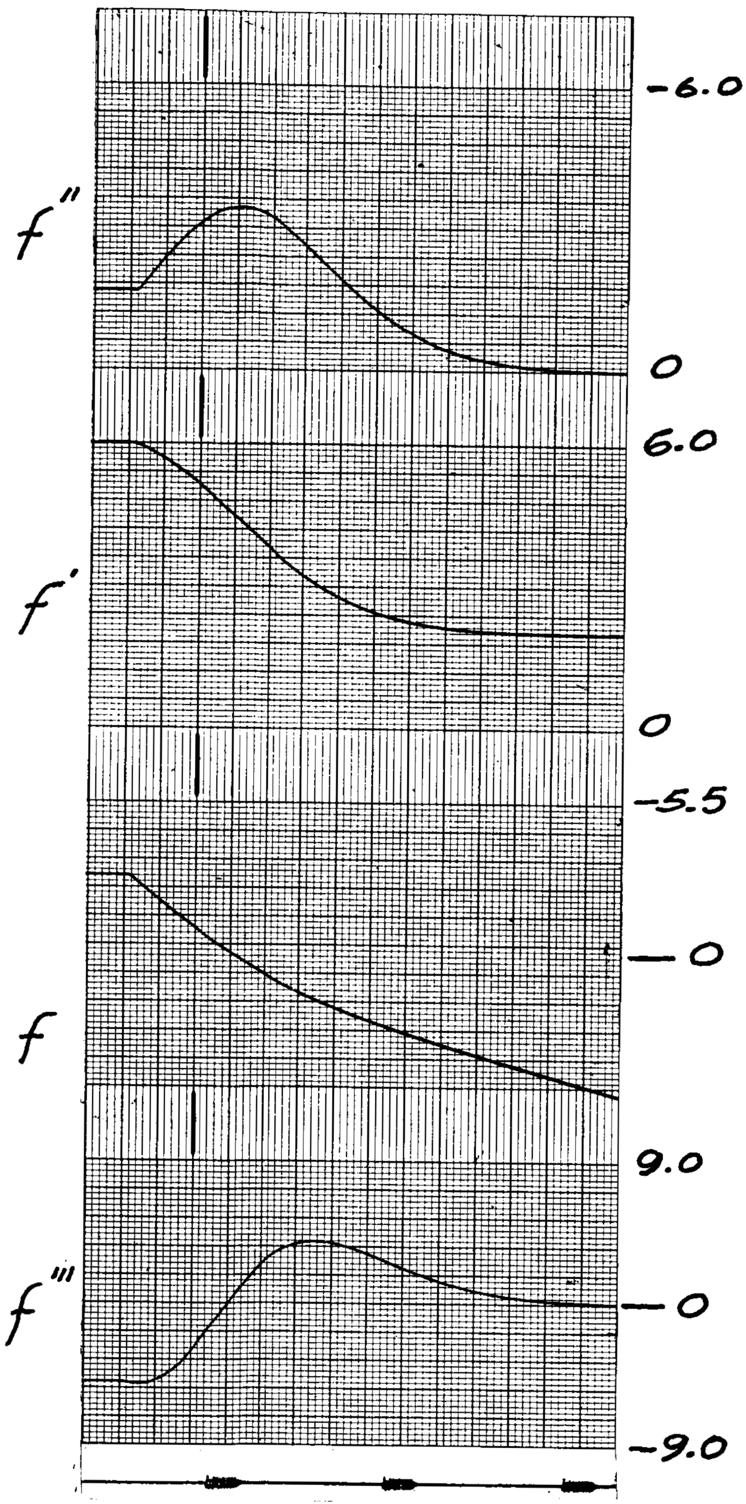

Fig. 5. (Continued)

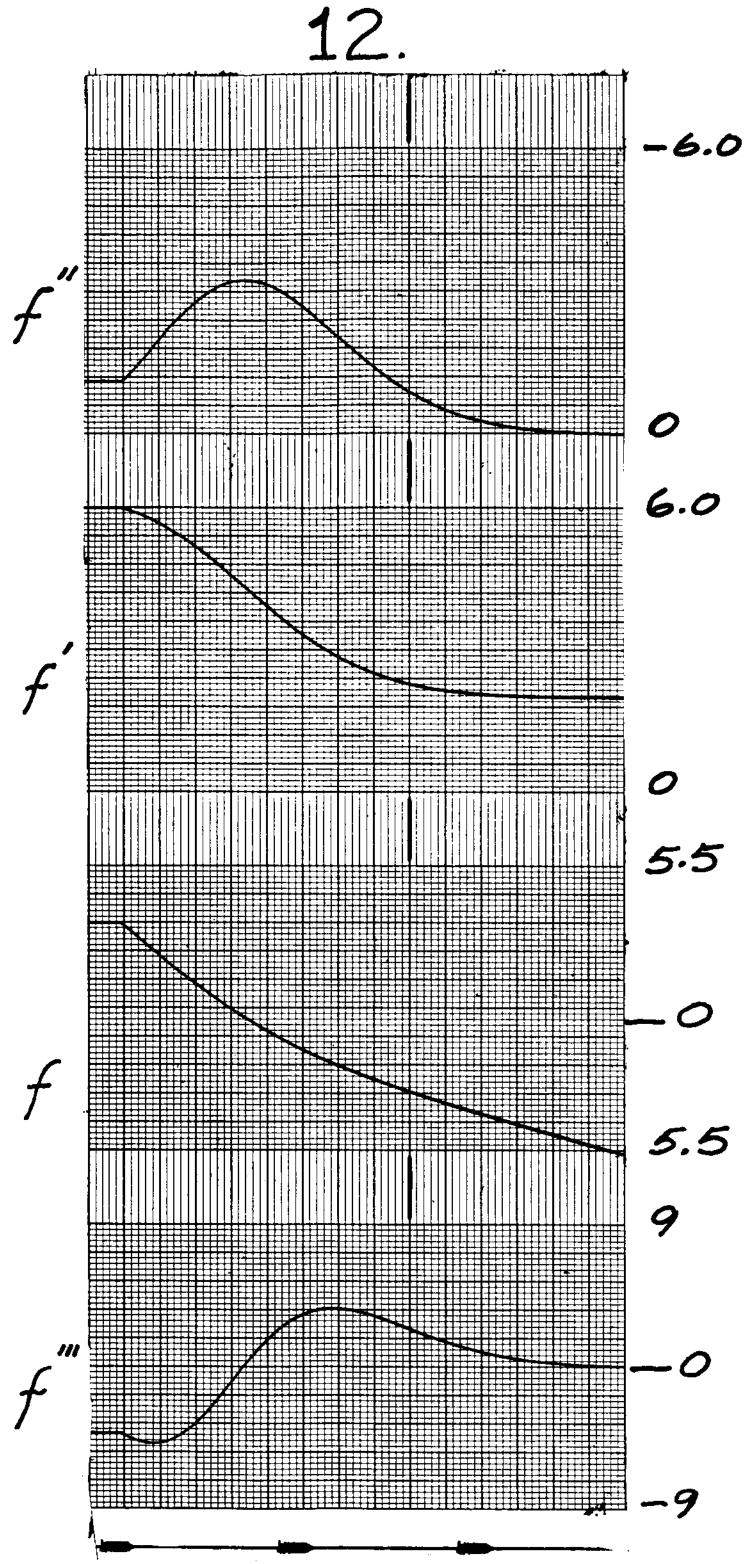

Fig. 5. (Continued)

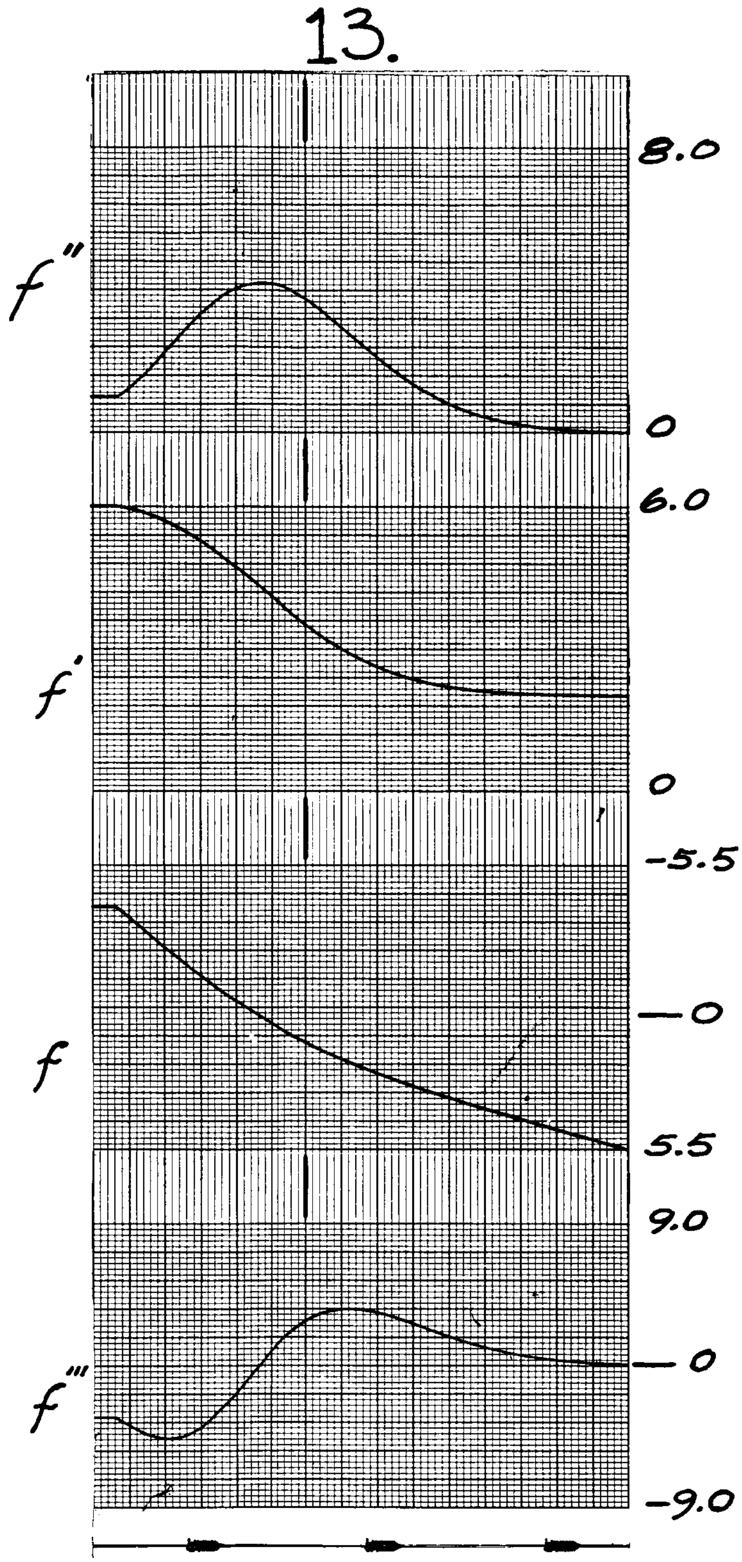

Fig. 5. (Continued)

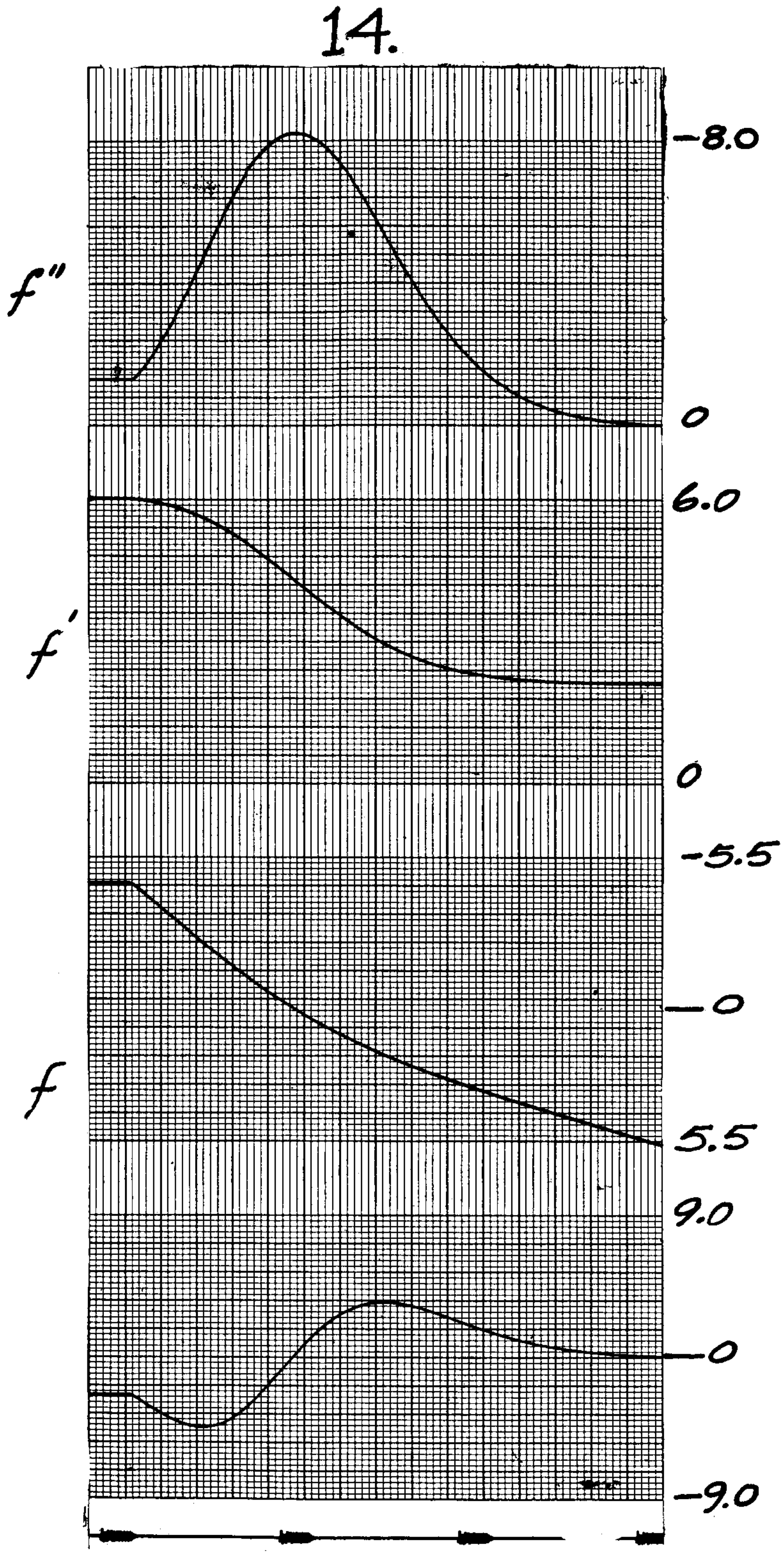

Fig. 5. (Continued)

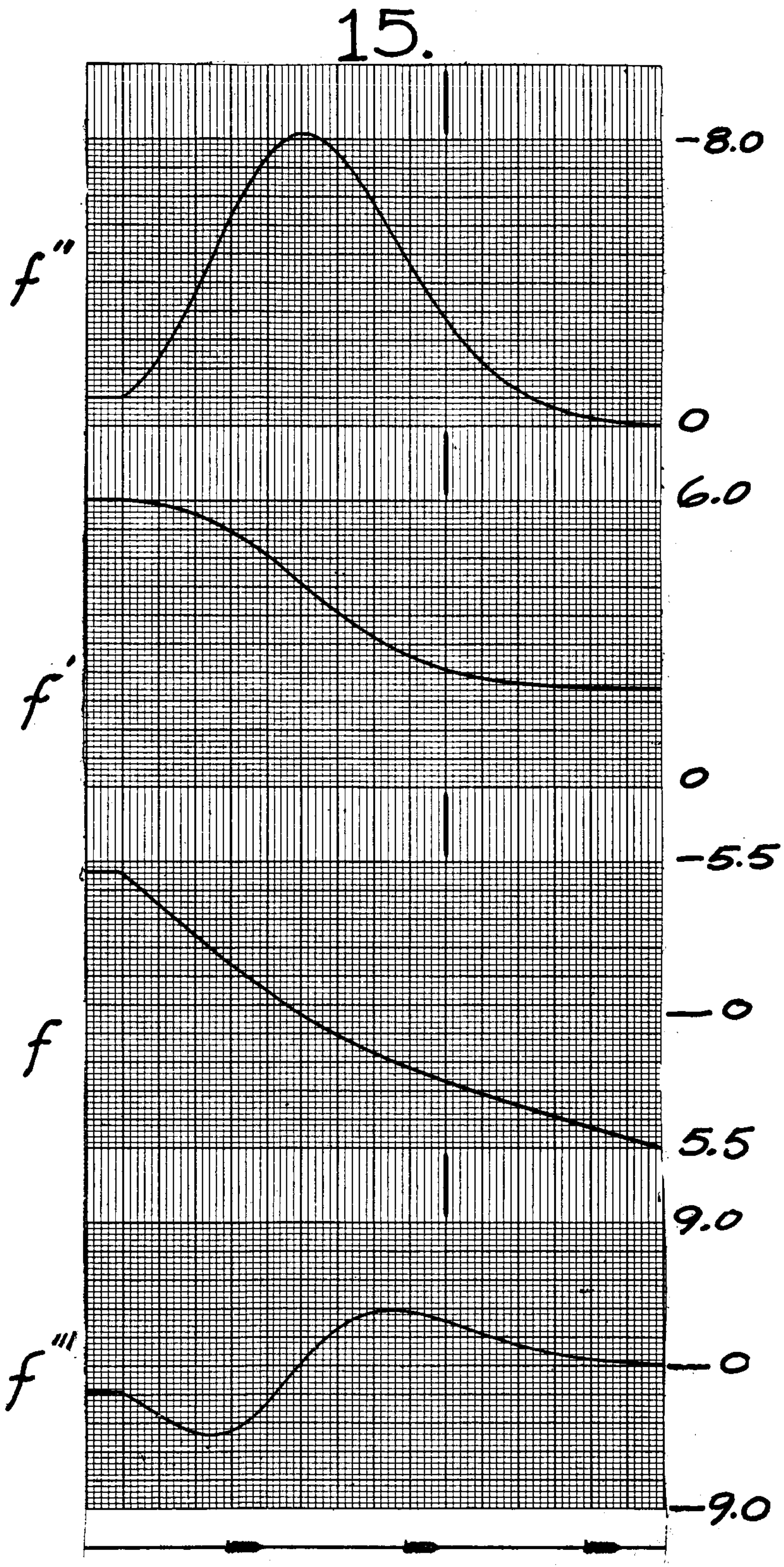

Fig. 5. (Continued)

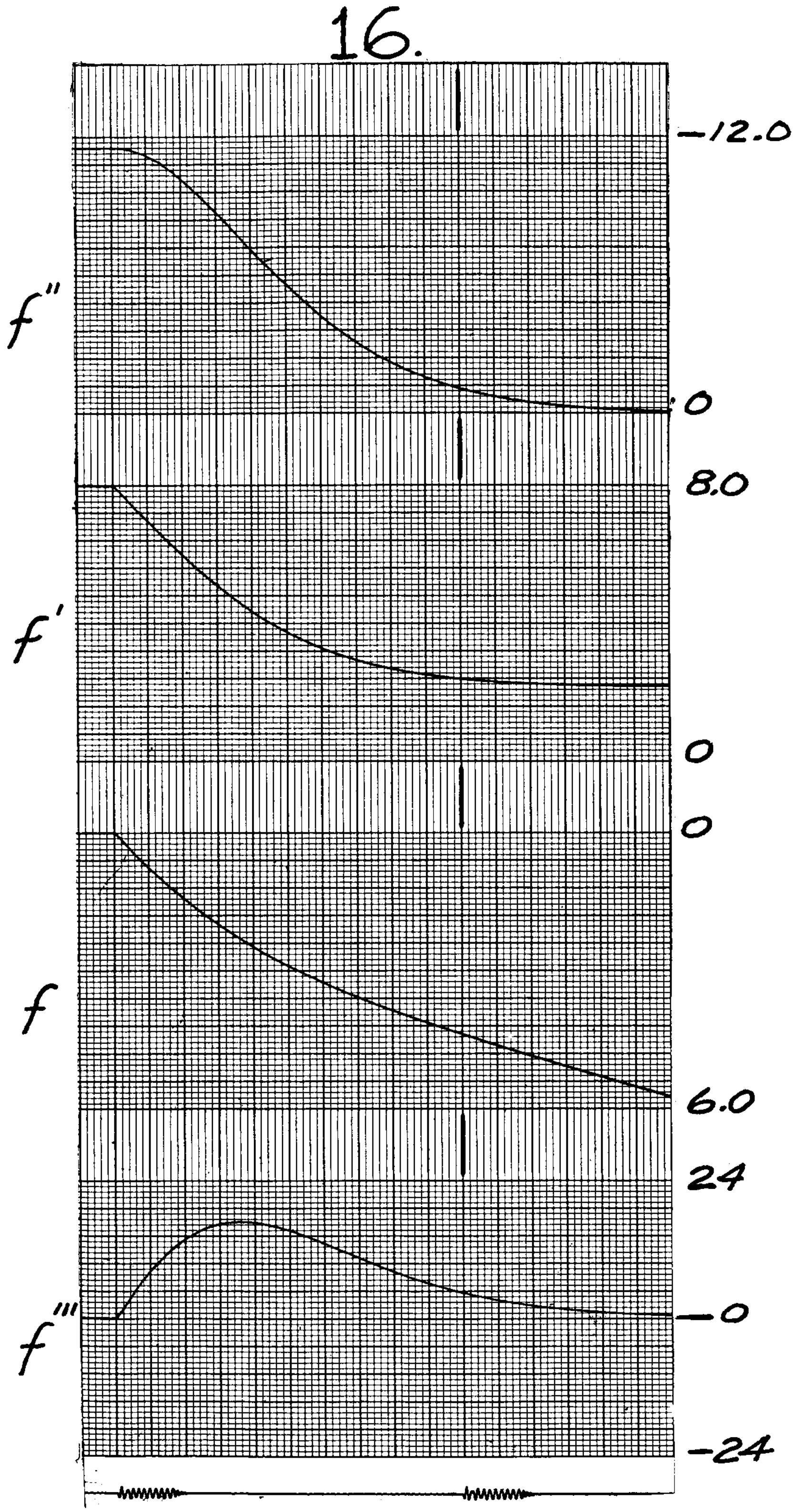

Fig. 5. (Continued)

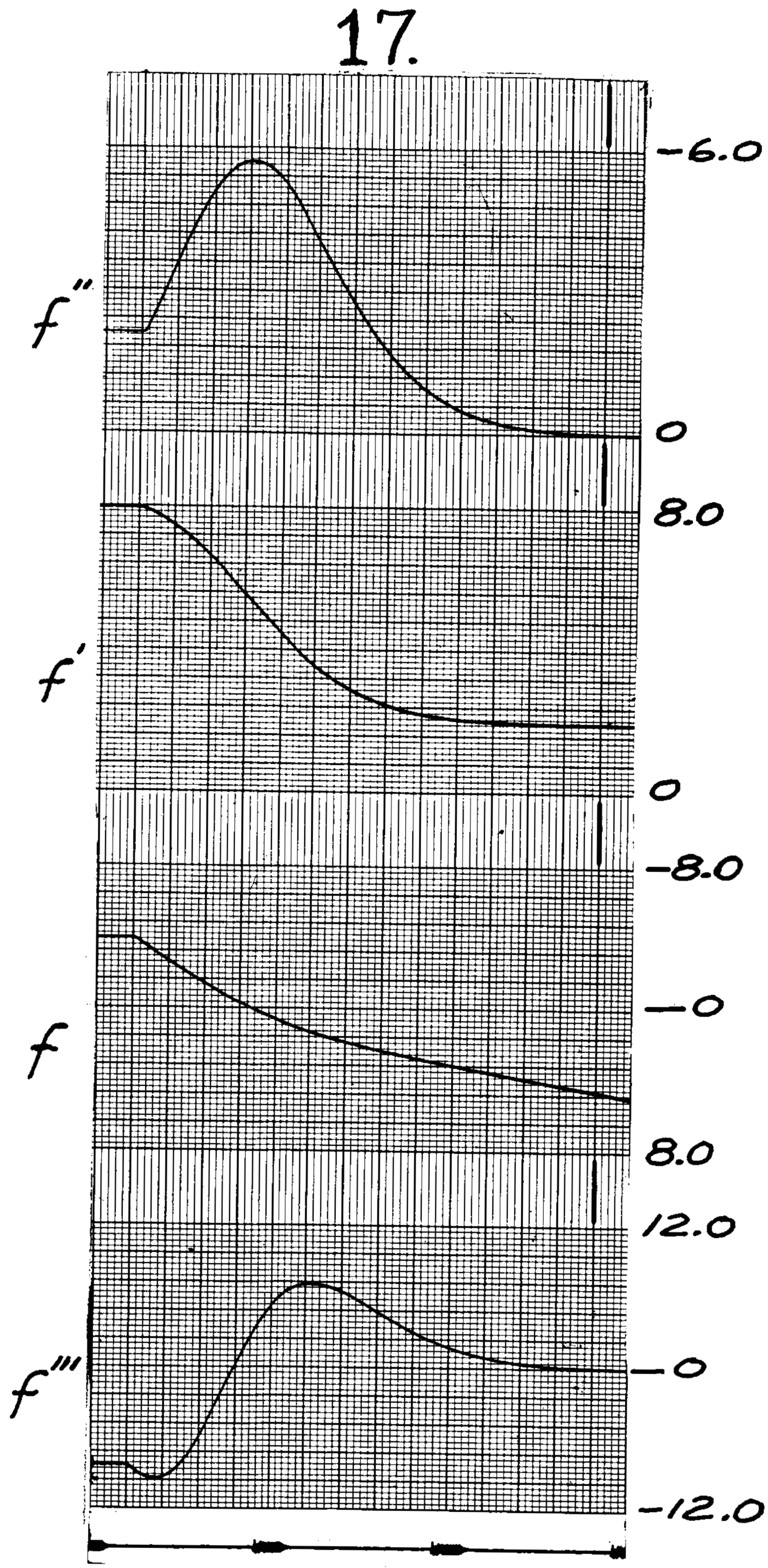

Fig. 5. (Continued)

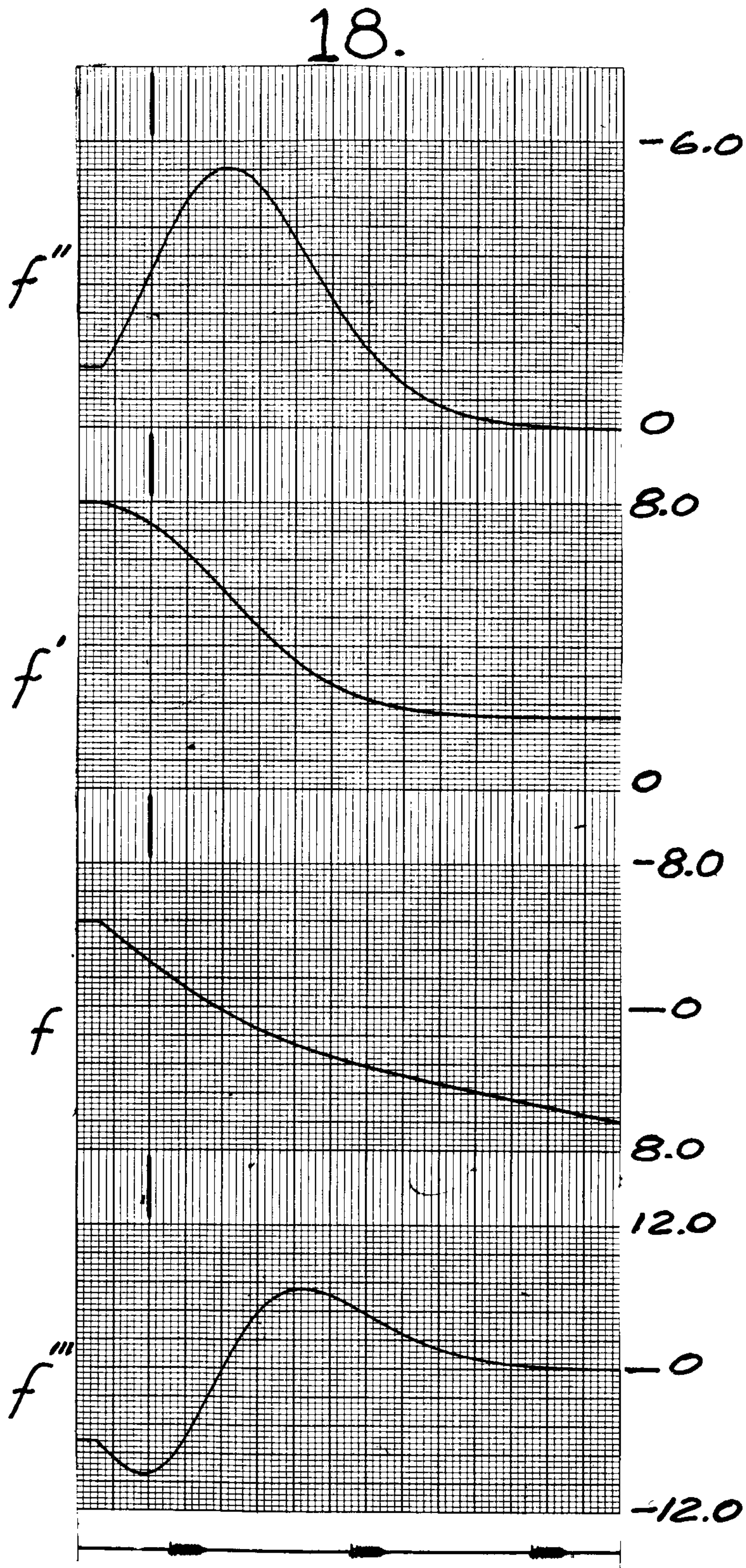

Fig. 5. (Continued)

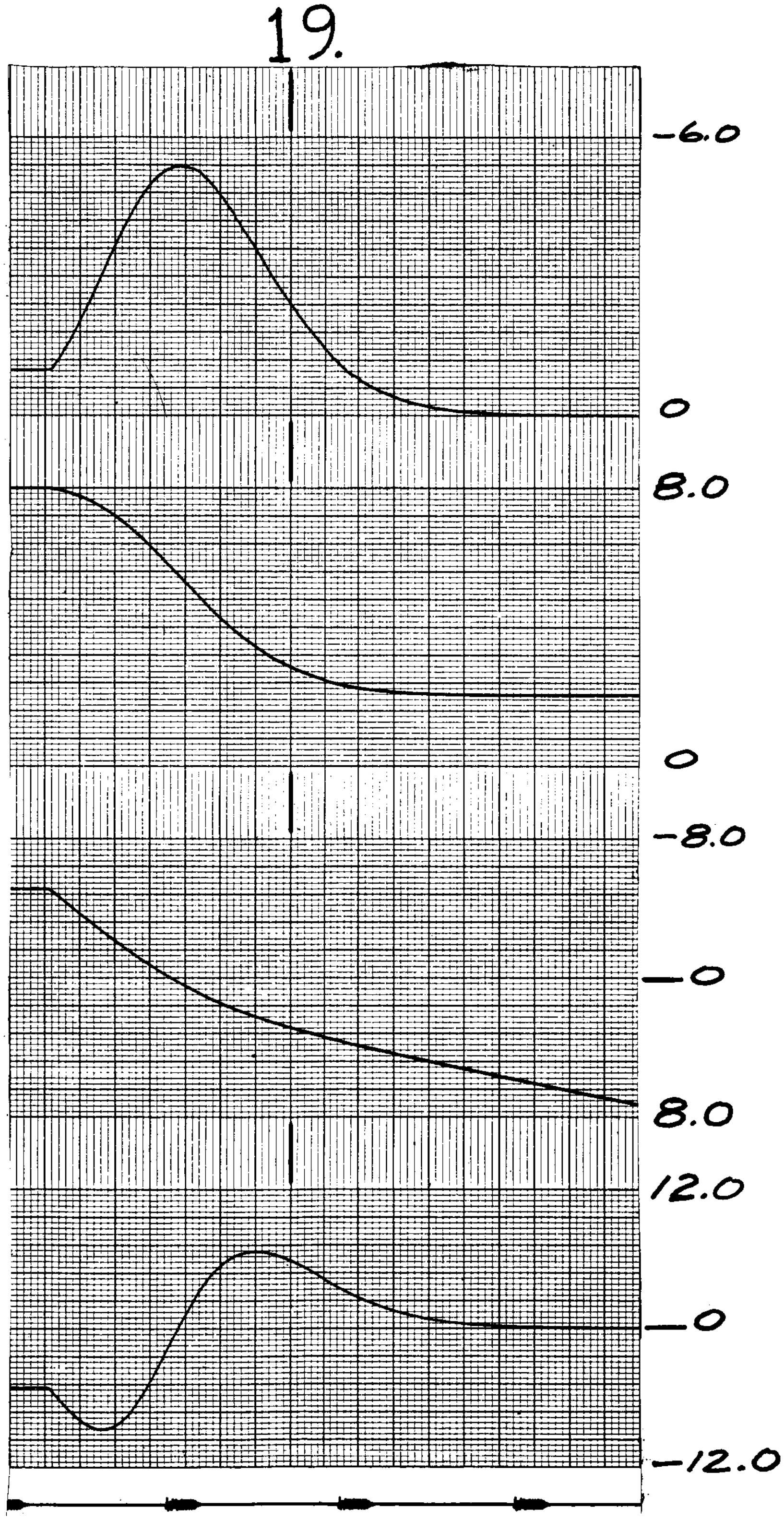

Fig. 5. (Continued)

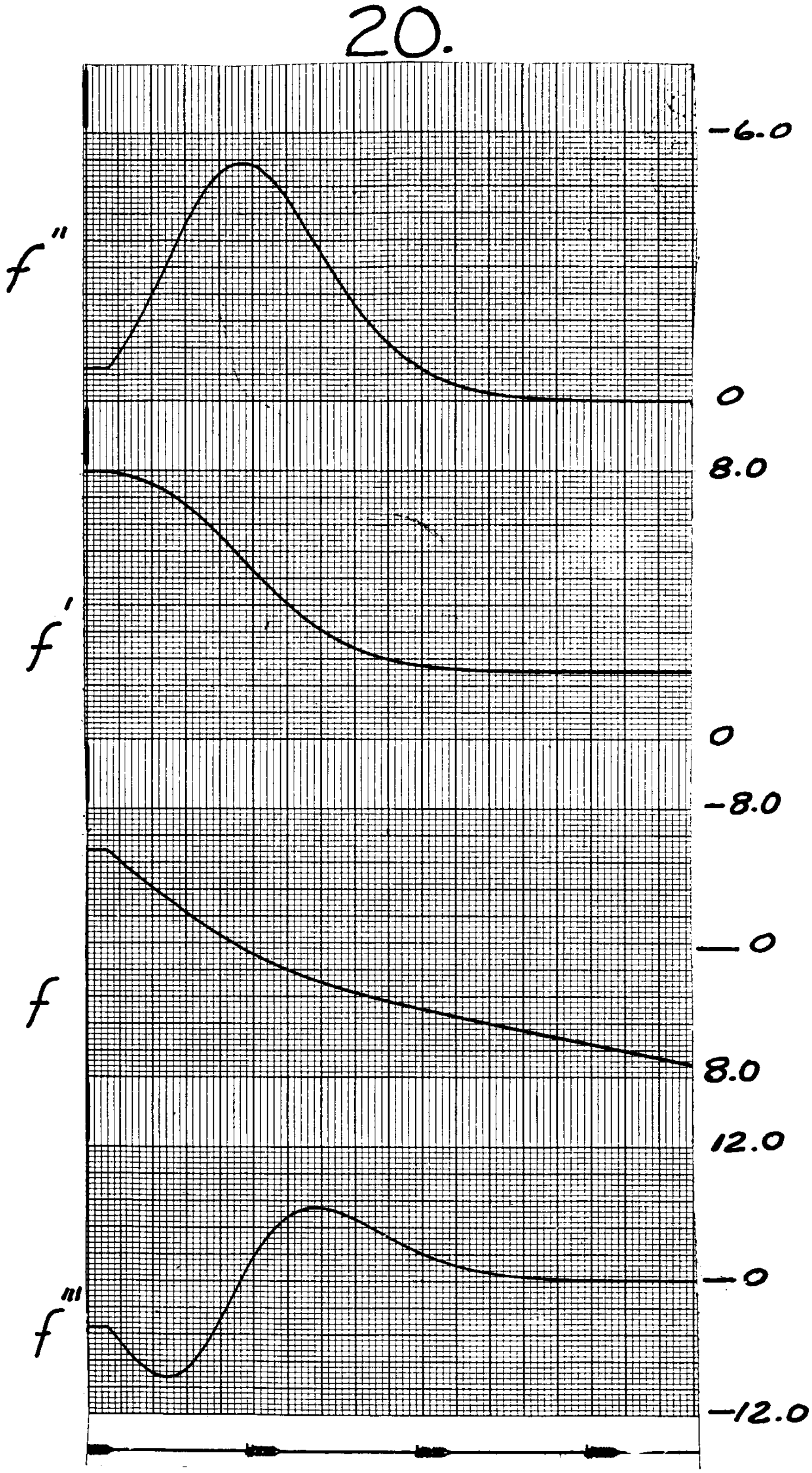

Fig. 5. (Continued)

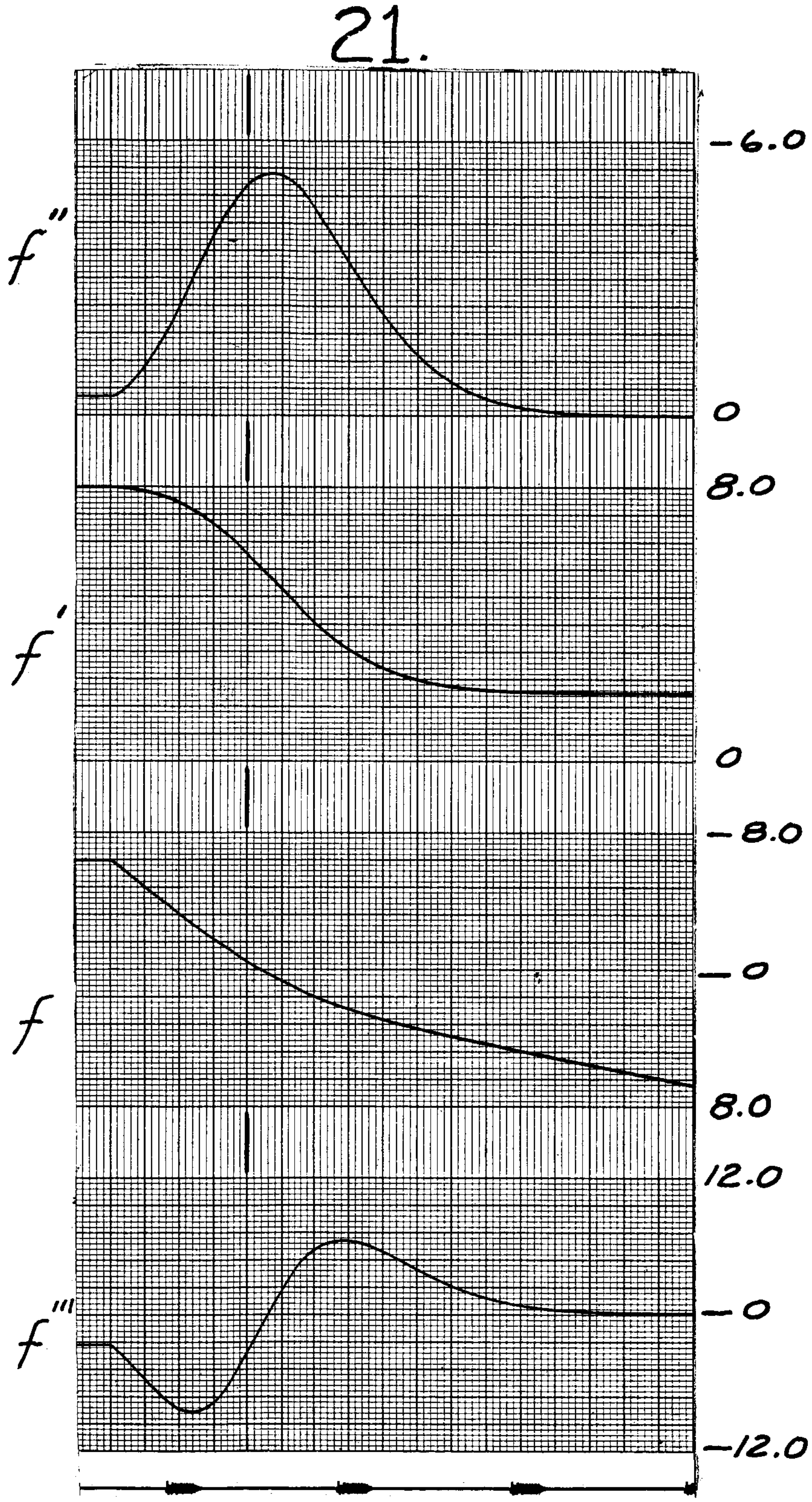

Fig. 5. (Continued)

22.

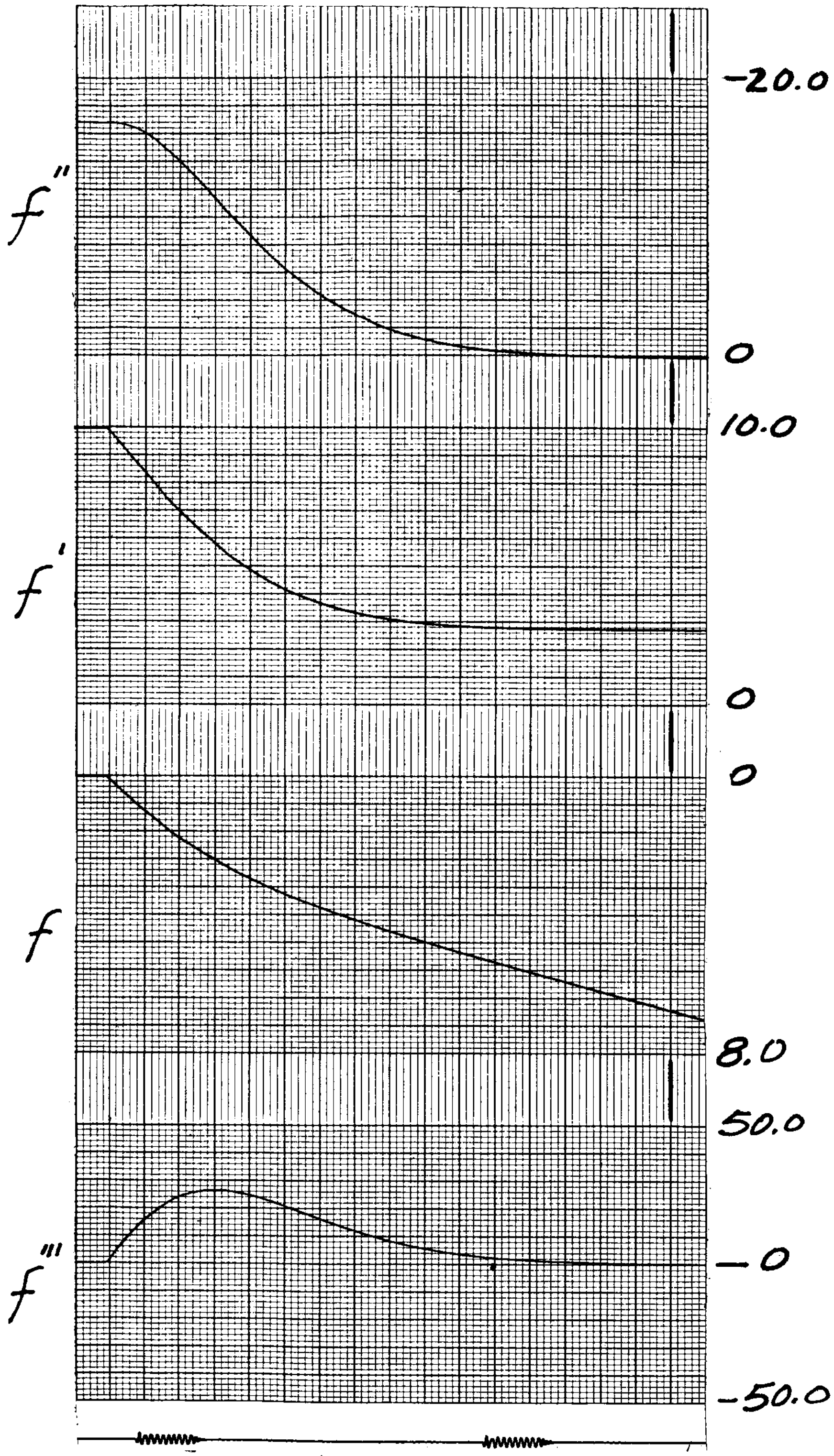

Fig. 5. (Continued)

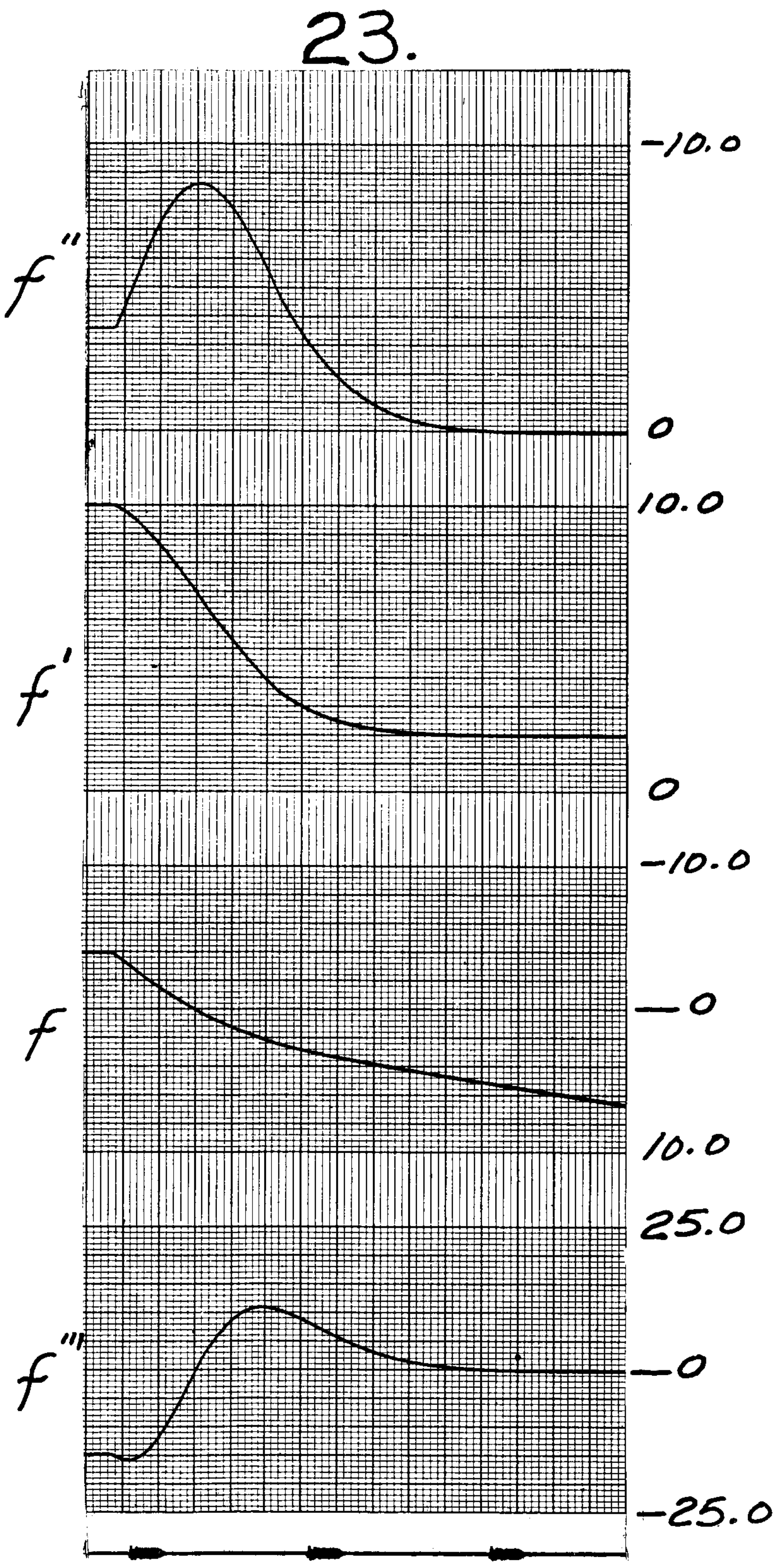

Fig. 5. (Continued)

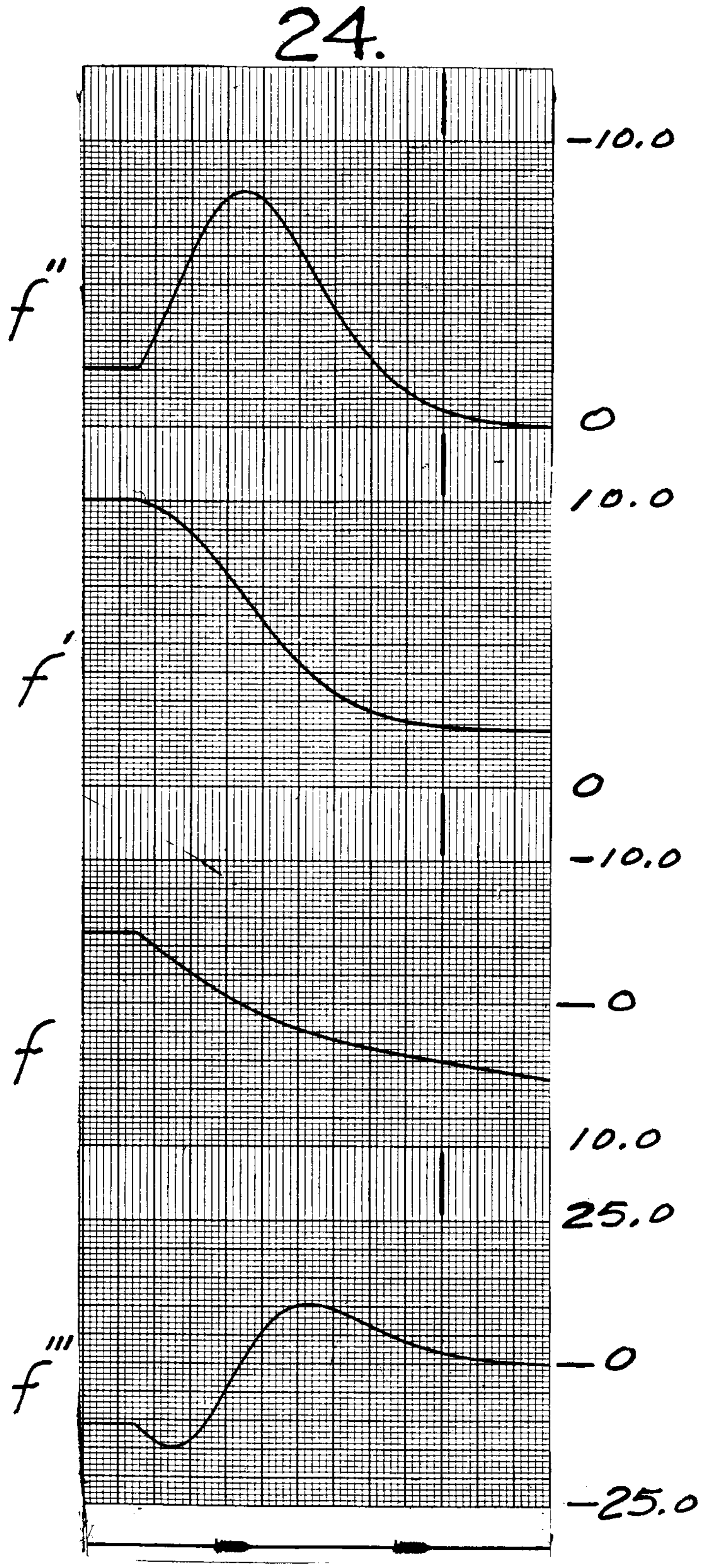

Fig. 5. (Continued)

25.

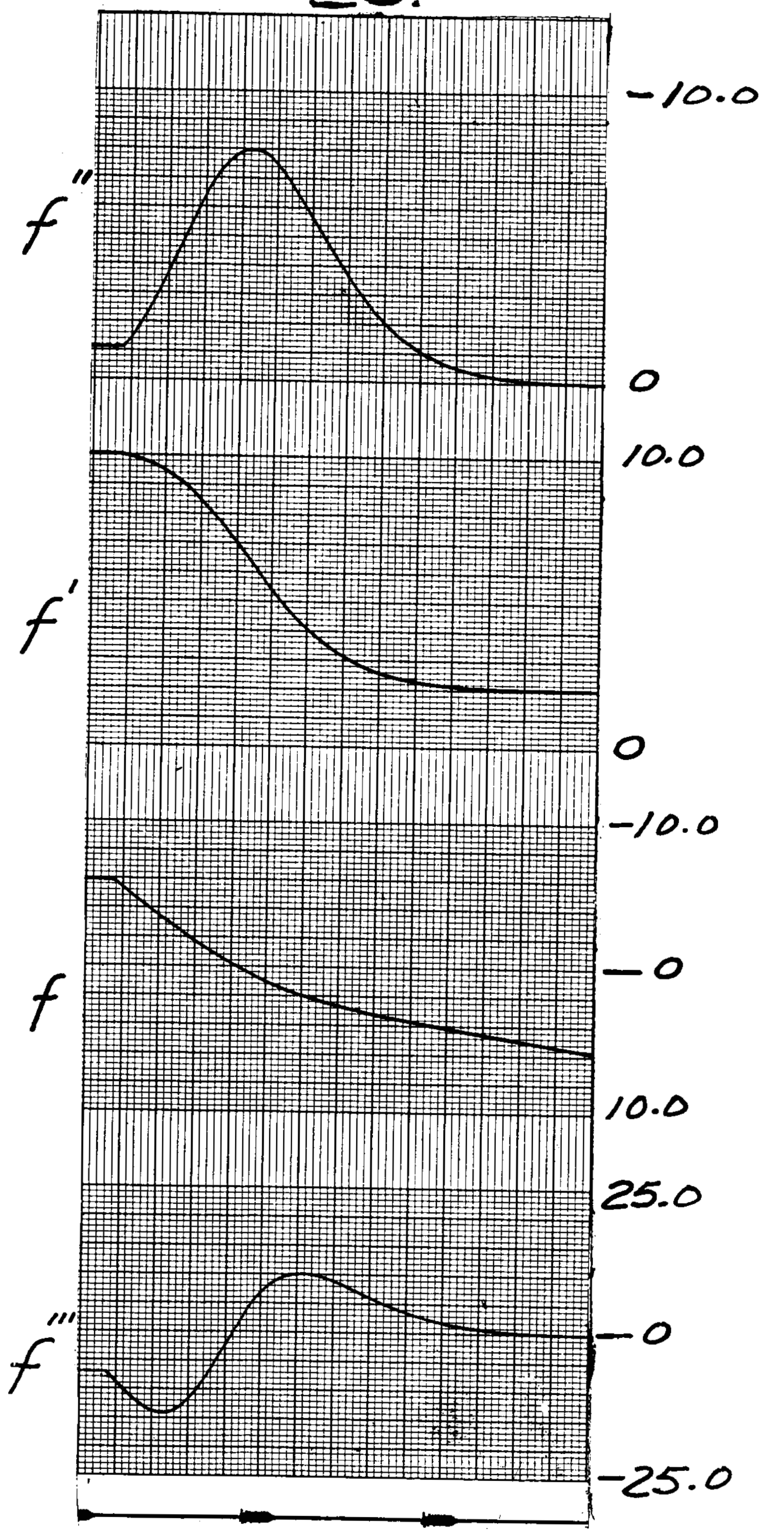

Fig. 5. (Continued)

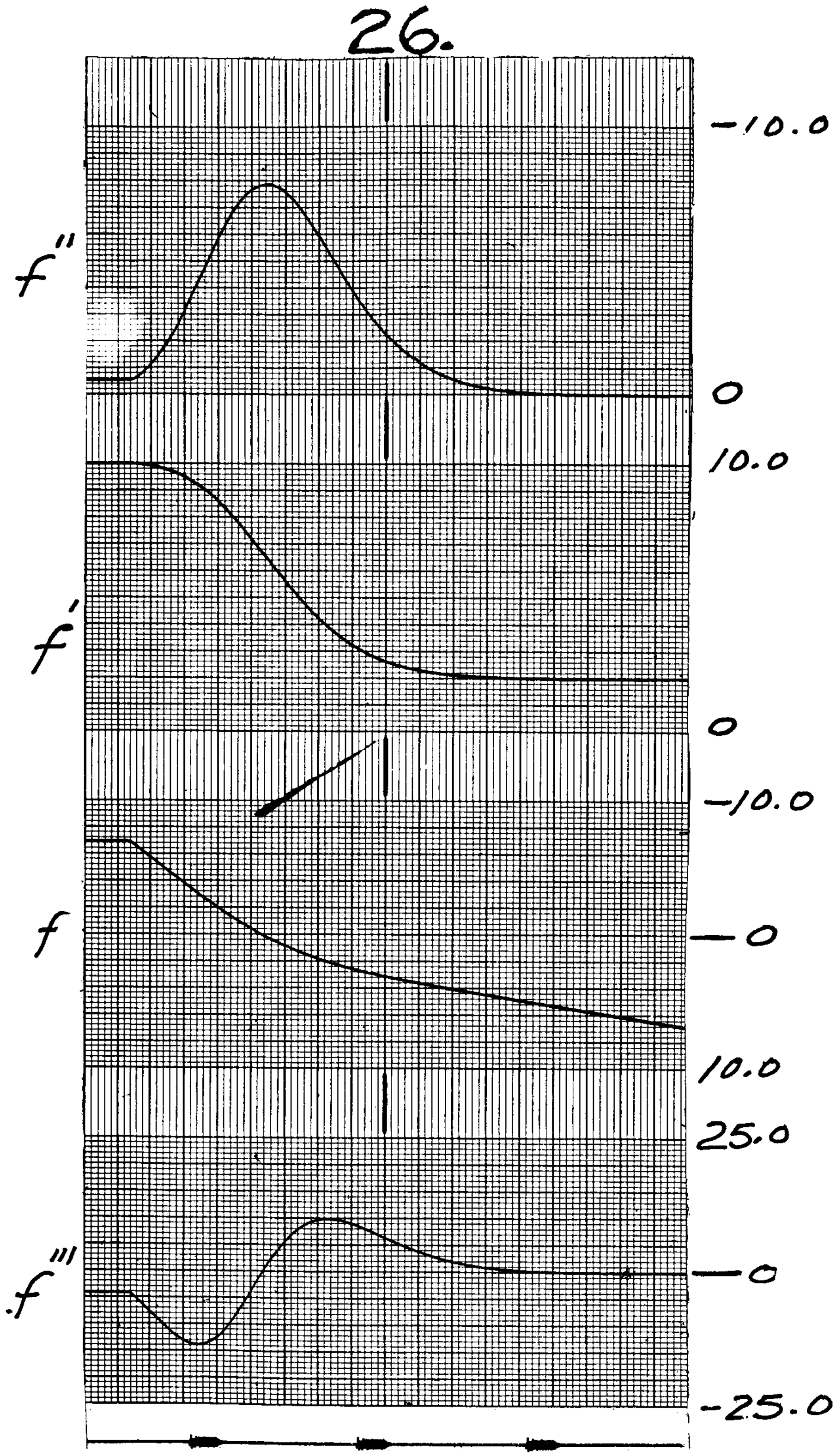

Fig. 5. (Continued)

27.

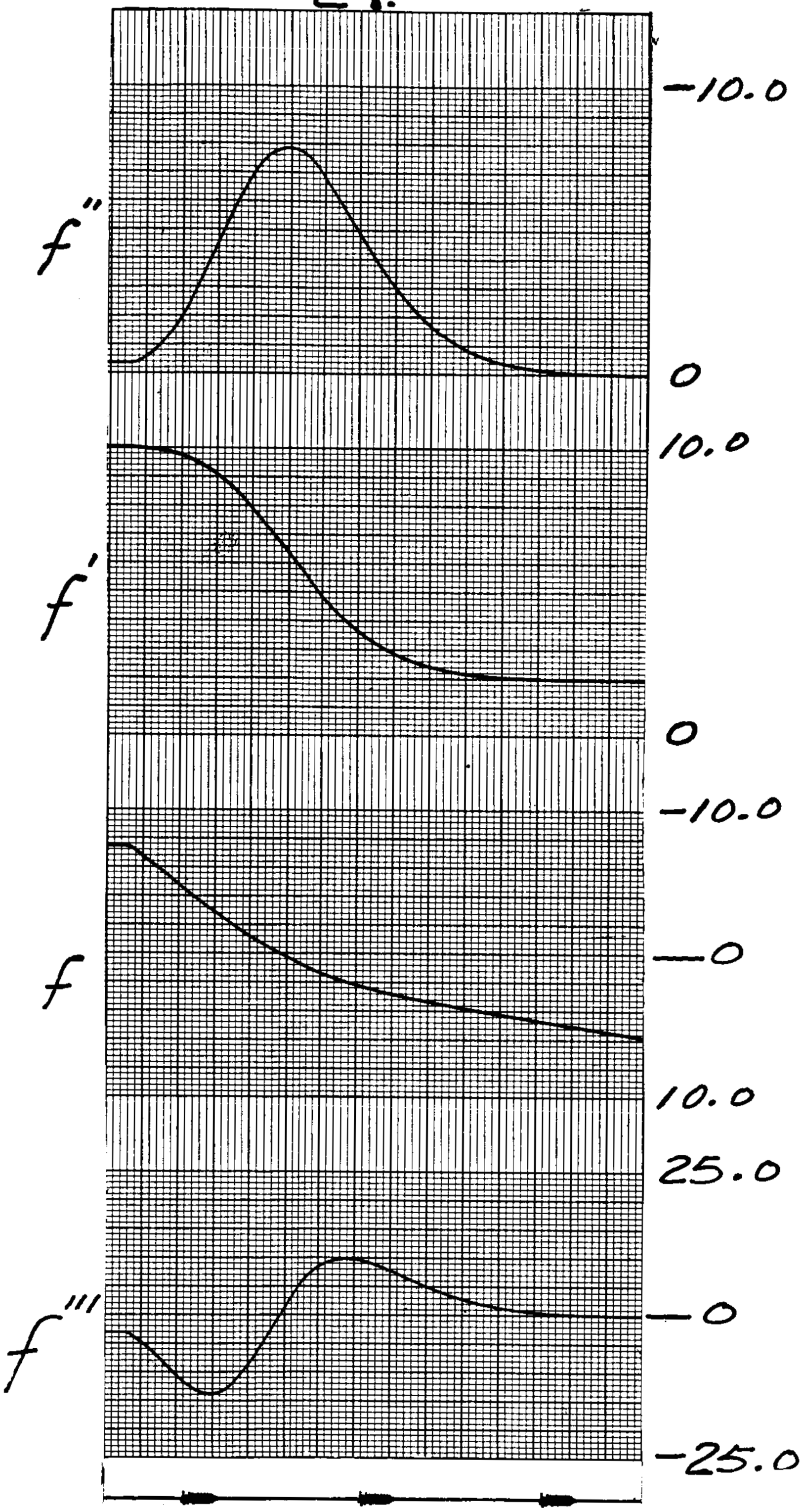

Fig. 5. (Concluded)

REFERENCES

1. Nicholls, J. A., Dabora, E. K., and Ragland, K. W., "A Study of Two Phase Detonation as it Relates to Rocket Motor Combustion Instability," NASA Contractor Report NASA CR-272, August 1965.

2. Dabora, E. K., Ragland, K. W., Ranger, A. A., and Nicholls, J. A., "Two Phase Detonations and Drop Shattering Studies," Univ. of Mich. ORA Report 06324-2-T, April 1966.

3. Dabora, E. K., Ragland, K. W., Ranger, A. A., and Nicholls, J. A., "Two Phase Detonations and Drop Shattering Studies," 3rd Annual Progress Report, NASA CR-7225, ORA 06324 3-T, March 1967.

4. Gordeev, V. E., Komov, V. F., and Troshin, Ya. K., "Concerning Detonation Combustion in Heterogeneous Systems," Proceedings of the Academy of Science, USSR, Vol. 160, No. 4 (Physical Chemistry), 1965.

5. Blasius, H., "Grenzschichten in Flussigkeiten mit kleiner Reibung," Z. Math. u. Phys., 56, 1 (1908).

6. Emmons, H. W. and Leigh, D. C., "Tabulation of the Blasius Function with Blowing and Suction," Aeronautical Research Council Current Paper No. 157, London, 1954.

7. Mirels, H., "Laminar Boundary Layer Behind Shock Advancing into Stationary Fluid," NACA TN 3401, March 1955.

8. Williams, F. A., Combustion Theory, Addison-Wesley, 1965.

9. Lees, L., "Convective Heat Transfer," Combustion and Propulsion, Third AGARD Colloquim, Pergamon Press, 1958, p. 451.

10. Glass, I. I. and Hall, G. J., Handbook of Supersonic Aerodynamics, Section 18, Shock Tubes, NAVORD Report 1488, Vol. 6, Dec. 1959, p. 332.

DISTRIBUTION LIST

NASA Lewis Research Center
21000 Brookpark Road
Cleveland, Ohio 44135
Attention: B.J. Clark (3)

NASA Lewis Research Center
21000 Brookpark Road
Cleveland, Ohio 44135
Attention: Library (2)

National Aeronautics and Space
Administration
Washington, D.C. 20546
Attention: Office of Grants and
Contracts (10)

NASA Goddard Space Flight Center
Greenbelt, Md. 20771
Attention: Library

Jet Propulsion Laboratory
4800 Oak Grove Dr.
Pasadena, Calif. 91103
Attention: Library

NASA Manned Spacecraft Center
Houston, Texas 77001
Attention: Library

NASA Western Operations
150 Pico Blvd.
Santa Monica, Calif. 90406
Attention: Library

Applied Physics Laboratory
The Johns Hopkins University
Attn: W.G. Berl
8621 Georgia Avenue
Silver Spring, Maryland 20910

Princeton University
Forrestal Campus
Guggenheim Laboratories
Attn: I. Glassman
Princeton, New Jersey 08540

NASA Scientific and Technical
Information Facility
Box 5700
Bethesda, Md.
Attention NASA Representative (6)

NASA Lewis Research Center
21000 Brookpark Road
Cleveland, Ohio 44135
Attention: Report Control Office

NASA Ames Research Center
Moffett Field, Calif. 94035
Attention: Library

NASA Flight Research Center
P.O. Box 273
Edwards, Calif. 93523
Attention: Library

NASA Langley Research Center
Langley Station
Hampton, Va. 23365
Attention: Library

NASA Marshall Space Flight Center
Huntsville, Ala. 35812
Attention: Library

Chemical Propulsion Information Agency
Attn: T.W. Christian
8621 Georgia Avenue
Silver Spring, Maryland 20910

University of Southern California
Dept. of Mechanical Engineering
Attn: M. Gerstein
University Park
Los Angeles, California 90007

Rocketdyne
A Div. of North American Aviation
Attn: E.C. Clinger
6633 Canoga Avenue
Canoga Park, California 91304

NASA
Lewis Research Center
Attn: E.W. Conrad
21000 Brookpark Road
Cleveland, Ohio 44135

U.S. Naval Ordnance Test Station
Attn: D. Couch
China Lake, California 93555

Multi-Tech., Inc.
Attn: F.B. Cramer
601 Glenoaks Blvd.
San Fernando, California 91340

Aerospace Corporation
Attn: O.W. Dykema
P.O. Box 95085
Los Angeles, California 90045

Ohio State University
Dept. of Aeronautical and Astronautical Engineering
Attn: R. Edse
Columbus, Ohio 43210

TRW Systems
Attn: G.W. Elverum
1 Space Park
Redondo Beach, California 90278

University of Illinois
Aeronautical and Astronautical Engineering
Urbana, Illinois
Attn: R.A. Strehlow

NASA
Headquarters
Attn: R.S. Levine, Code RPL
6th and Independence Ave, S.W.
Washington, D.C. 20546

Pratt and Whitney Aircraft
Florida Research & Development Ctr.
Attn: G.D. Lewis
P.O. Box 2691
West Palm Beach, Florida 33402

Defense Research Corporation
Attn: B. Gray
P.O. Box 3587
Santa Barbara, California 93105

Research and Technology Division
Air Force Systems Command
Attn: L. Green, Jr. (RTGS)
Bolling AFB, Washington, D.C. 20332

Princeton University
Forrestal Campus
Guggenheim Laboratories
Attn: D. Harrje
Princeton, New Jersey 08540

Aerojet-General Corporation
Attn: R.J. Hefner
P.O. Box 15847
Sacramento, California 95809

Dynamic Science Corporation
Attn: R.J. Hoffman
1900 Walker Avenue
Monrovia, California 91016

Office of Naval Research
Navy Department
Attn: R.D. Jackel, 429
Washington, D.C. 20360

Rocketdyne
A Div. of North American Aviation
Attn: R.B. Lawhead
6633 Canoga Avenue
Canoga Park, California 91304

NASA
Lewis Research Center
Attn: R.J. Priem, MS-86-5
21000 Brookpark Road
Cleveland, Ohio 44135

Sacramento State College
Engineering Division
Attn: F.H. Reardon
60000 J. Street
Sacramento, California 95189

Thiokol Chemical Corporation
Reaction Motors Division
Attn: D. Mann
Denville, New Jersey 07834

Dartmouth University
Attn: P.D. McCormack
Hanover, New Hampshire 03755

University of Wisconsin
Mechanical Engineering Department
Attn: P.S. Myers
1513 University Avenue
Madison, Wisconsin 53705

University of California
Department of Chemical Engineering
Attn: A.K. Oppenhiem
6161 Etcheverry Hall
Berkeley, California 94720

Purdue University
School of Mechanical Engineering
Attn: J.R. Osborn
Lafayette, Indiana 47907

United Technology Center
Attn: R.H. Osborn
P.O. Box 358
Sunnyvale, California 94088

U.S. Naval Ordnance Test Station
Attn: E.W. Price, Code 508
China Lake, California 93555

Massachusetts Institute of Technology
Department of Mechanical Engineering
Attn: T.Y. Toong
Cambridge, Massachusetts 02139

Illinois Institute of Technology
RM 200 M.H.
Attn: T.P. Torda
3300 S. Federal Street
Chicago, Illinois 60616

NASA
George C. Marshall Space Flight Center
R-P&VE-PA, Attn: R.J. Richmond
Huntsville, Alabama 35812

Bell Aerosystems Company
Attn: T.G. Rossmann
P.O. Box 1
Buffalo, New York 14205

Jet Propulsion Laboratory
California Institute of Technology
Attn: J.H. Rupe
4800 Oak Grove Drive
Pasadena, California 91103

University of California
Mechanical Engineering, Thermal Sys.
Attn: R. Sawyer
Berkeley, California 94720

ARL (ARC)
Attn: K. Scheller
Wright-Patterson AFB
Dayton, Ohio 45433

NASA Manned Spacecraft Center
Attn: J.G. Thibadaux
Houston, Texas 77058

Geophysics Corporation of America
Technology Division
Attn: A.C. Tobey
Burlington Road
Bedford, Massachusetts 01730

AFRPL (RPRR)
R.R. Weiss
Edwards, California 93523

U.S. Army Missile Command
AMSMI-RKL, Attn: W.W. Wharton
Redstone Arsenal, Alabama 35808

The Warner & Swasey Company
Control Instrument Division
Attn: R.H. Tourin
32-16 Downing Street
Flushing, New York 11354

United Aircraft Corporation
Research Labs.
Attn: D.H. Utvick
400 Main Street
East Hartford, Connecticut 06108

General Electric Company
Schnectady, New York
Attn: D.R. White

Air Force Office of Scientific Research
Attn: B.T. Wolfson
1400 Wilson Blvd.
Arlington, Virginia 22209

Georgia Institute of Technology
Aerospace School
Attn: B.T. Zinn
Atlanta, Georgia 30332